Electronic Supplementary Material (ESI) for Green Chemistry.

Spruce Bark Stilbenes as a Nature-inspired Sun Blocker for Sunscreens

Dou Jinze[1*], Sui Mengmeng[1], Malinen, Kiia[1]; Pesonen Terhi[2], Isohanni Tiina[2], Vuorinen Tapani[1]

[1]Department of Bioproducts and Biosystems, Aalto University, Espoo, Finland

[2]Lasikuja 2, Lumene Oy, Espoo, Finland

Fig. S1. Photographs of the original non-modified finished sunscreen lotion (base-L, left 1), SPF 15-L (left 2), SPF 30-L (left 3), and SPF 15-B (left 4).

Table S1. The product ingredients of sunscreen E-II-1% and E-II-2%.

	composition	**%**
water phase (B)	AQUA (WATER)	ca. 70%
	GLYCERIN	
	BETULA ALBA (BIRCH) JUICE	
	HUMECTANTS	
	PRESERVATIVES, CHELATING AGENTS	
	XANTHAN GUM	
oil phase (C)	CETEARYL ALCOHOL	ca. 10 %
	CETYL PALMITATE	
	SODIUM STEAROYL GLUTAMATE	
	HYDROXYETHYL ACRYLATE/SODIUM ACRYLOYLDIMETHYL TAURATE COPOLYMER	
	PHENOXYETHYL CAPRYLATE	
	DIMETHICONE	
	OTHER OIL SOLUBLE INGREDIENTS	
water phase (A)	SPRUCE BARK EXTRACT	1 % or 2%
	HEAT SENSITIVE CARING INGREDIENTS + OTHER ADDITIVES	ca. 19 %
pH adjustment	NaOH	pH 6.8-7.2

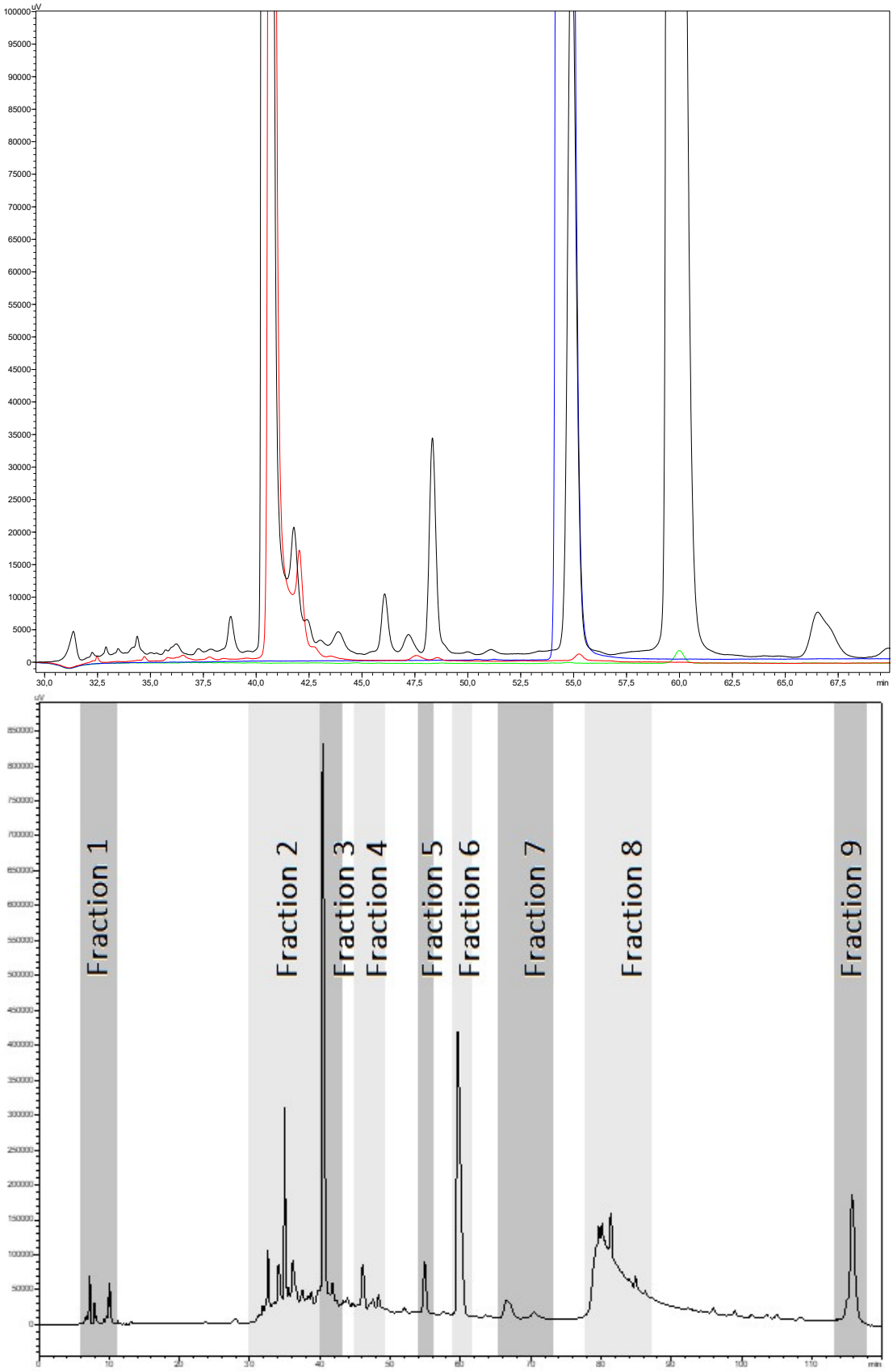

Fig. S2. 1) The HPLC chromatogram (30 - 70 min) from spruce bark extract and standard compounds (black = spruce bark extract, red = astringin, blue = polydatin and green = isorhapontin) at wavelength of 320 nm; 2) The HPLC chromatogram from spruce bark extract at wavelength of 210 nm with collected fractions for further chemical profile study using the **column set I** (**Table S2**).

Table S2. Summarized retention time of the semi-preparative scale purification and HPLC-DAD-MS analysis. The analysts elute out in a relative manner although the column size is different. ***** refers to approximated values.

	semi-preparative		HPLC-DAD-MS analytical	
Fraction	Retention time (min)	**Column set I**	Retention time (min)*****	**Column set II**
1	6.00 - 11.00	semi-preparative Luna® Omega 5 µm PS C18 100 Å (250 x 10 mm) column and Kinetex® 5 µm Biphenyl 100 Å (250 x 10 mm) column	1.5-2.50	analytical Phenomenex Luna® Omega 5 µm PS C18 100 Å (150x 2.1 mm) column and Kinetex® 5 µm Biphenyl 100 Å (150 x 2.1 mm) column
2	30.00 - 40.00		4.00-7.50	
3	40.01 – 42.50		20.50-21.50	
4	44.90 – 50. 00		-	
5	53.50 – 55.50		25.00-25.50	
6	58.20 – 61.80		26.50-27.50	
7	65.00 – 72.50		28.50-32.00	
8	77.50 – 87.50		38.50-40.00	
9	113.50- 117.50		105.00-110.50	

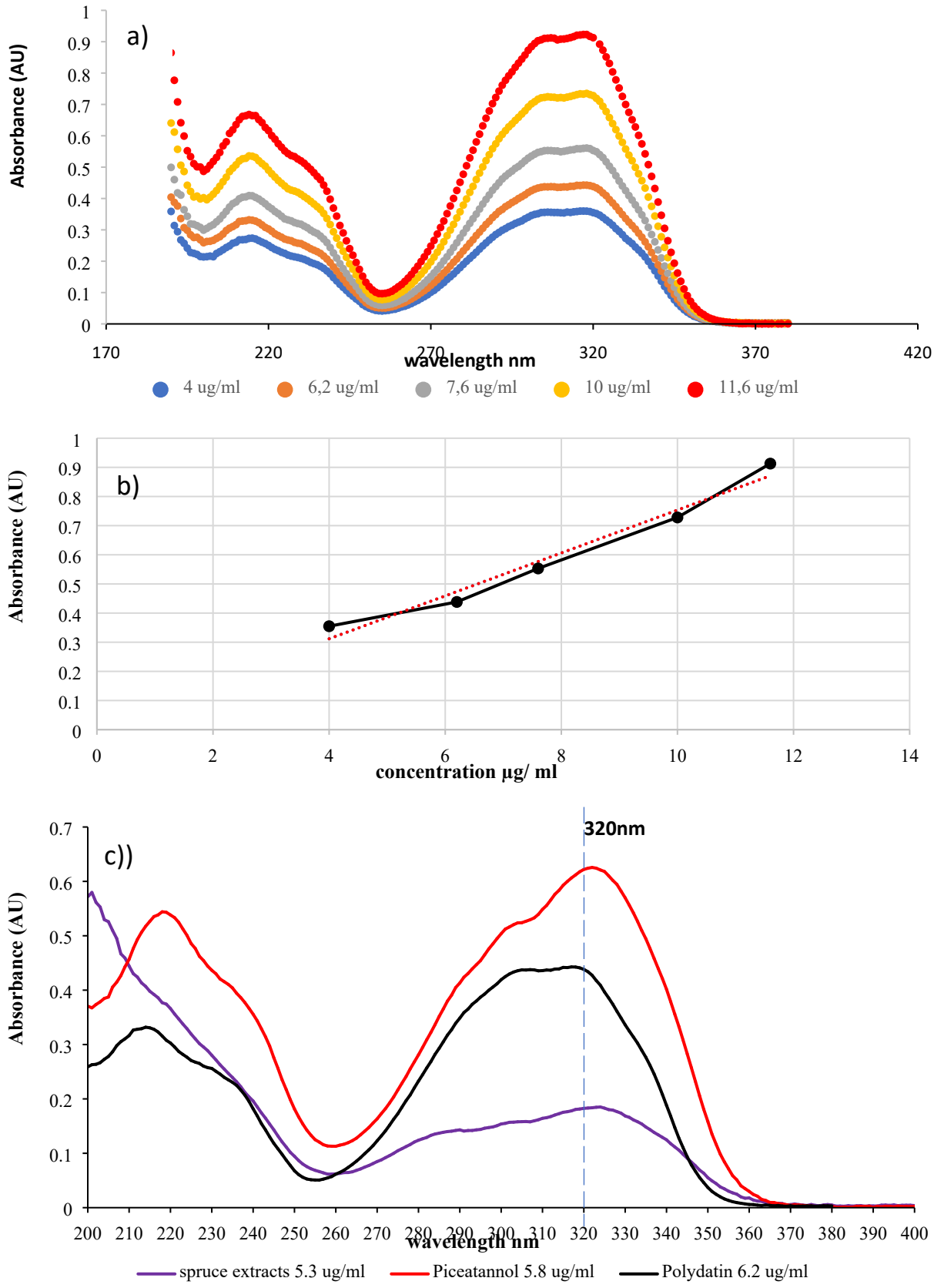

Fig. S3. a) The UV-vis spectra of polydatin solutions of various concentrations: 4, 6.2, 7.6, 10 and 11.6 µg/mL; b) Calibration curve for quantification of polydatin based on its absorption intensity at 320 nm; c) UV absorption spectra, measured with a Shimadzu UV-2550 spectrophotometer (Kyoto, Japan), of authentic piceatannol, polydatin together with Spruce bark Ethanol 60 v-% extract.

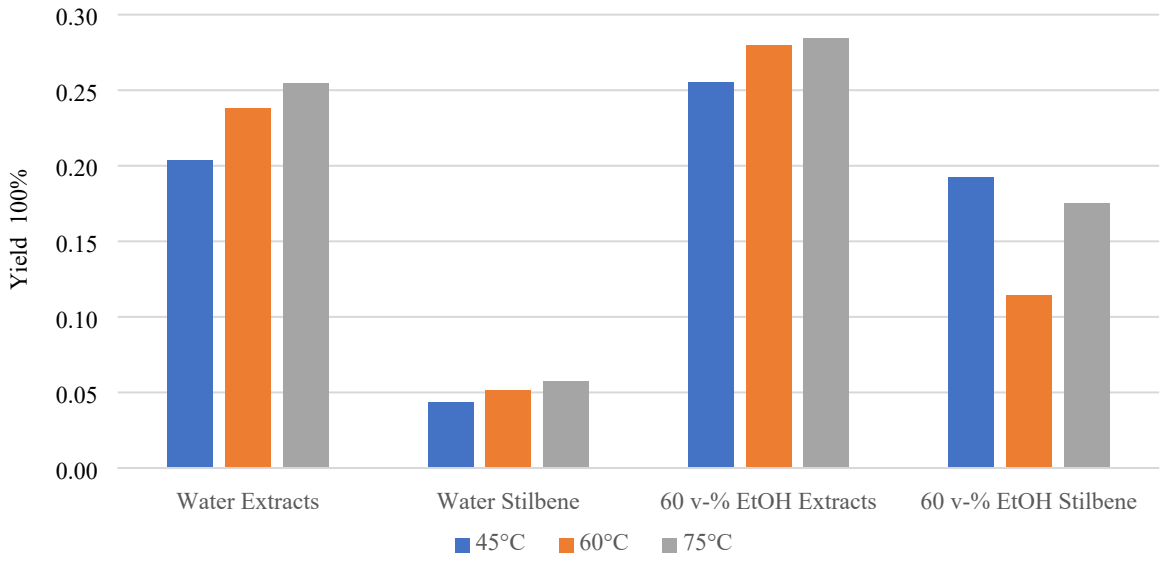

Fig. S4. The effect of the solvent (Ethanol 60 v-% and water) and temperature (45, 60 and 75 °C) on the overall yield of UAE extraction (E) and stilbene-like compounds (S). The extraction time was constant (i.e. 20 min). One independent experiment was performed.

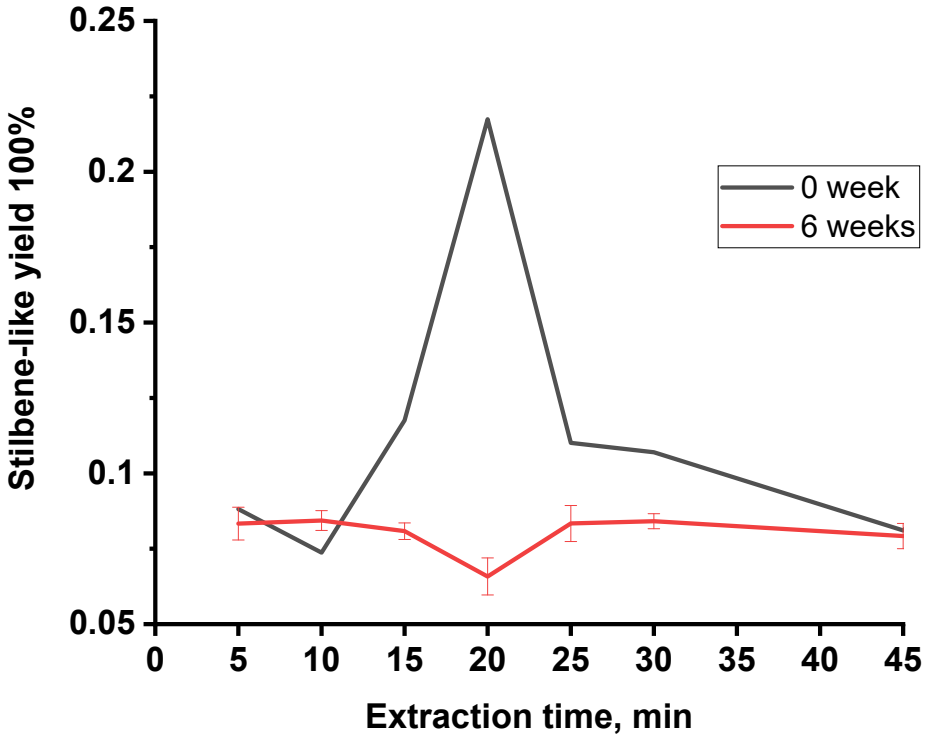

Fig. S5. The stability test of extracts (T 45 °C) that were prepared both freshly (0-week, one independent experiment) and 6 weeks (two independent experiments). UV-vis spectroscopy (at wavelength number of 320 nm) was applied here for the quantitation of the stilbene-like compounds.

Table S3. ^{1}H and ^{13}C NMR chemical shifts of the identified Astringin 1, Isorhapontin 2, and Polydatin 3 (see **Fig. 1**) from spruce UAE extracts at **Fig. 5**.

	Astringin 1	Isorhapontin 2	Polydatin 3
H-2’	7.06 (s)	7.22 (d, 1.51)	7.42 (d, 8.29)
H-8	7.11 (d, 16.3)	7.11 (d, 16.3)	7.11 (d, 16.28)
H-6’	equivalent to H-2’	6.99 (m)	equivalent to H-2’
H-7	6.93 (d, 24.0)	6.93 (d, 24.0)	6.93 (d, 16.41)
H-5’	6.85 (d, 9.31)	6.85 (d, 9.31)	6.85 (d, 8.21)
H-3'	equivalent to H-5’	—	equivalent to H-5’
H-2	6.83 (s)	6.83 (s)	6.82 (s)
H-6	6.69 (s)	6.69 (s)	6.69 (s)
H-4	6.50 (t)	6.50 (t)	6.50 (s)
H-1''	4.96 (7.46)	4.96 (7.46)	4.97 (d, 7.26)
CH_3O	—	3.81	—
OH-2"	5.58	5.58	5.59
OH-3"	5.39	5.39	5.37
OH-4"	5.3	5.3	5.29
OH-6"	4.88	4.88	4.89
H-6''a	3.82	3.82	3.86 (m)
H-6''b	3.54	3.54	3.63 (m)
H-5''	3.45	3.45	3.46 (m)
H-3''	3.42	3.42	3.41 (m)
H-2''	3.36 (m)	3.36 (m)	3.36 (m)
H-4''	3.33 (m)	3.33 (m)	3.33 (m)
C-3	159.1	159.1	159.1
C-5	158.6	158.6	158.6
C-4'	145.9	146.9	157.5
C-1'	139.5	139.5	139.5
C-1	128.6	128.6	128.6
C-8	129.1	129.1	128.1
C-7	125.3	125.6	125.3
C-6'	118.9	120.4	127.9
C-2'	113.5	110.1	same as C6'
C-3'	145.7	148.1	115.6
C-5'	115.9	115.7	same as C3'
C-6	107.3	107.5	107.3
C-2	105.1	105.1	104.8
C-4	102.9	103.1	102.9
C-1''	100.9	100.9	100.9
C-5''	77.3	77.3	77.3
C-3''	76.9	76.9	76.9
C-2''	73.4	73.5	73.5
C-4''	69.9	70	69.9
C-6''	60.9	60.9	60.9

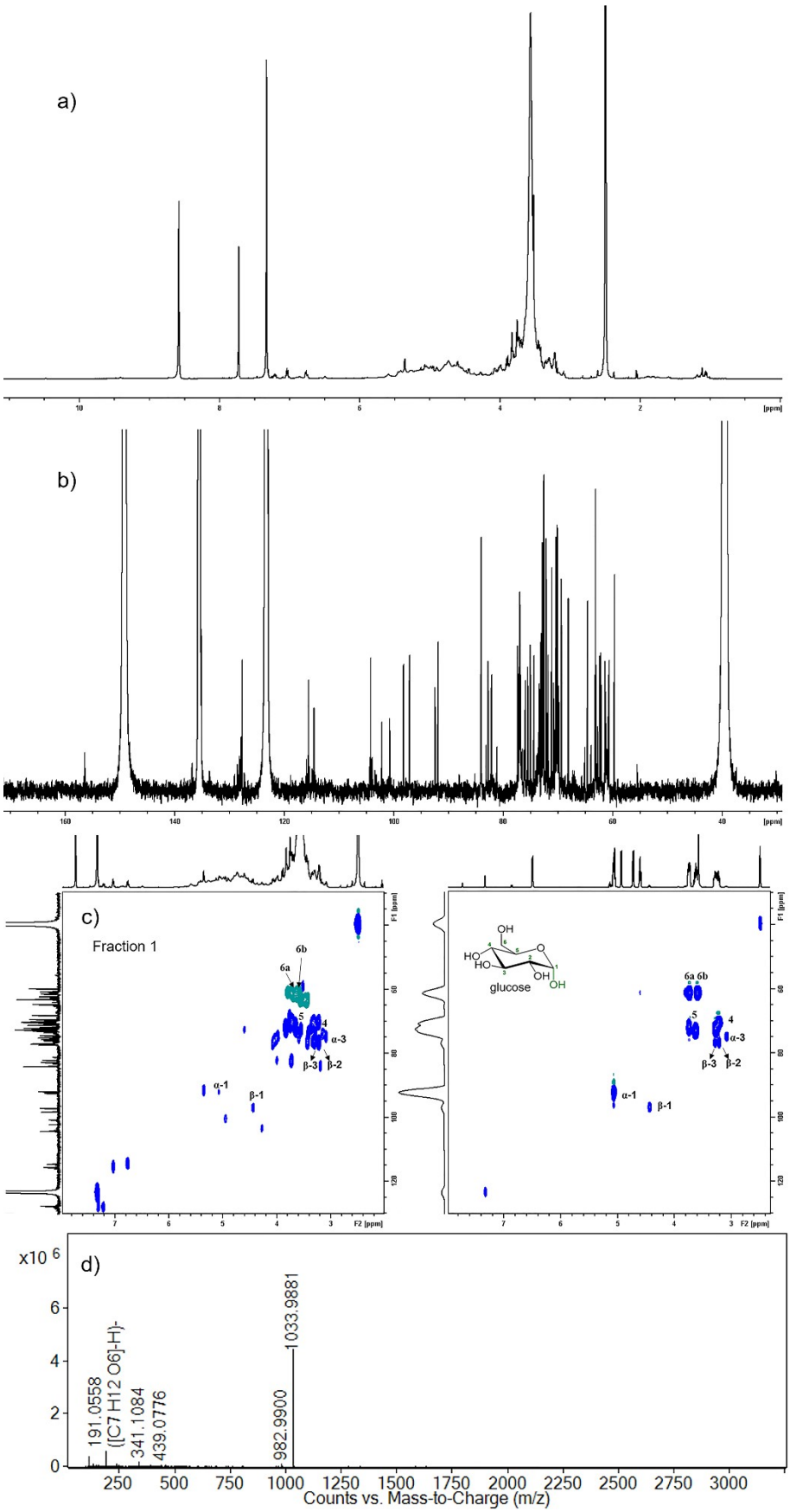

Fig. S6. a)^{1}H; b) ^{13}C of Fraction 1 (see **Fig. S2**); c) 2D ^{1}H–^{13}C HSQC NMR spectrum of Fraction 1 (see **Fig. S2**) and glucose in DMSO-*d*6/pyridine-*d*5; and d) HRMS spectrum (- ESI scan) of the Fraction 1 (see **Fig. S2**) using the **column set I**.

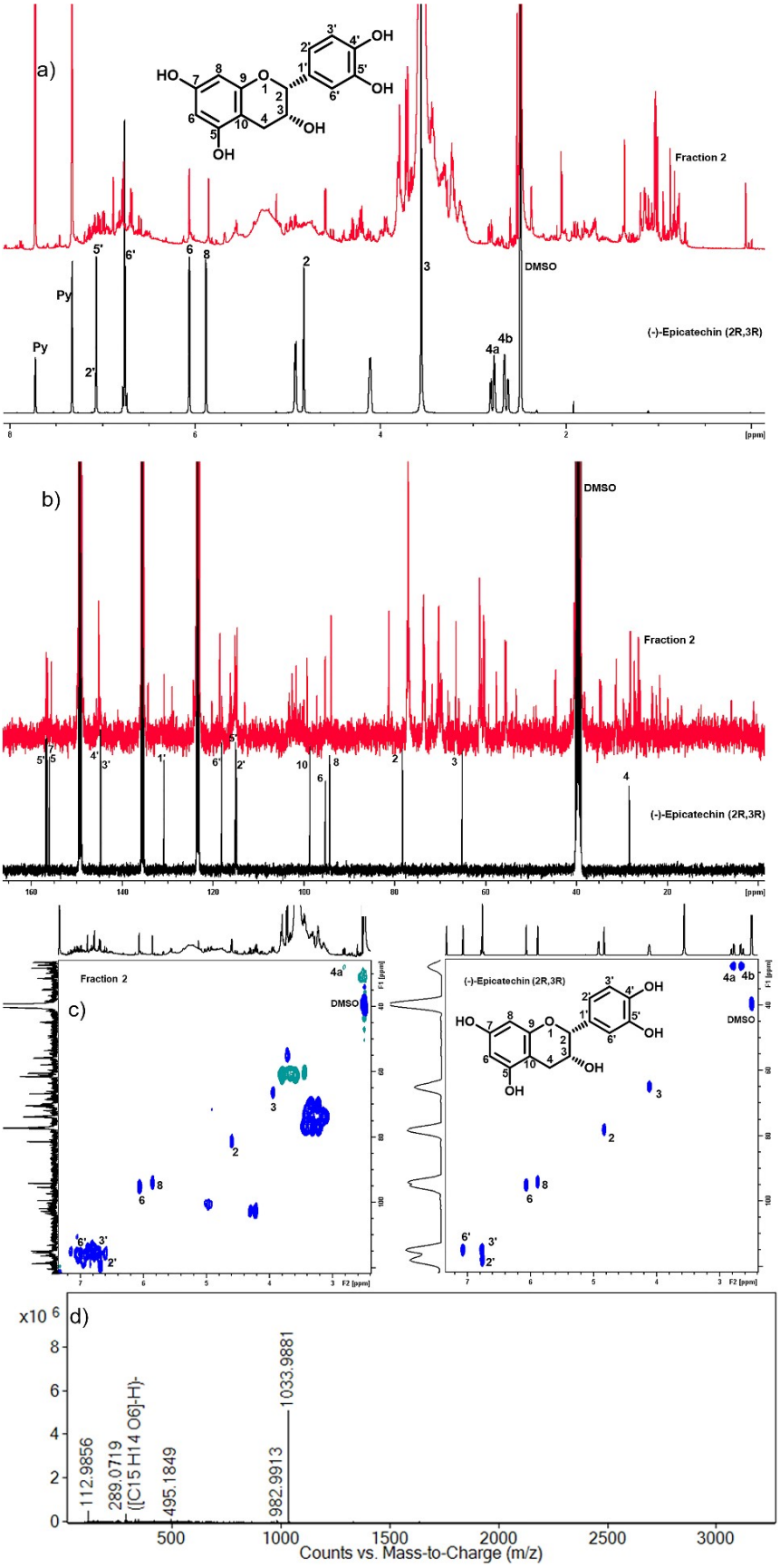

Fig. S7. a)^{1}H of Fraction 2; b) ^{13}C of **Fraction 2** (see **Fig. S2**) and Epicatechin; c) 2D ^{1}H–^{13}C HSQC NMR spectrum of **Fraction 2** (see **Fig. S2**) and Epicatechin in DMSO-*d*6/pyridine-*d*5; and d) HRMS spectrum (- ESI scan) of the **Fraction 2** (see **Fig. S2**) using the **column set I**.

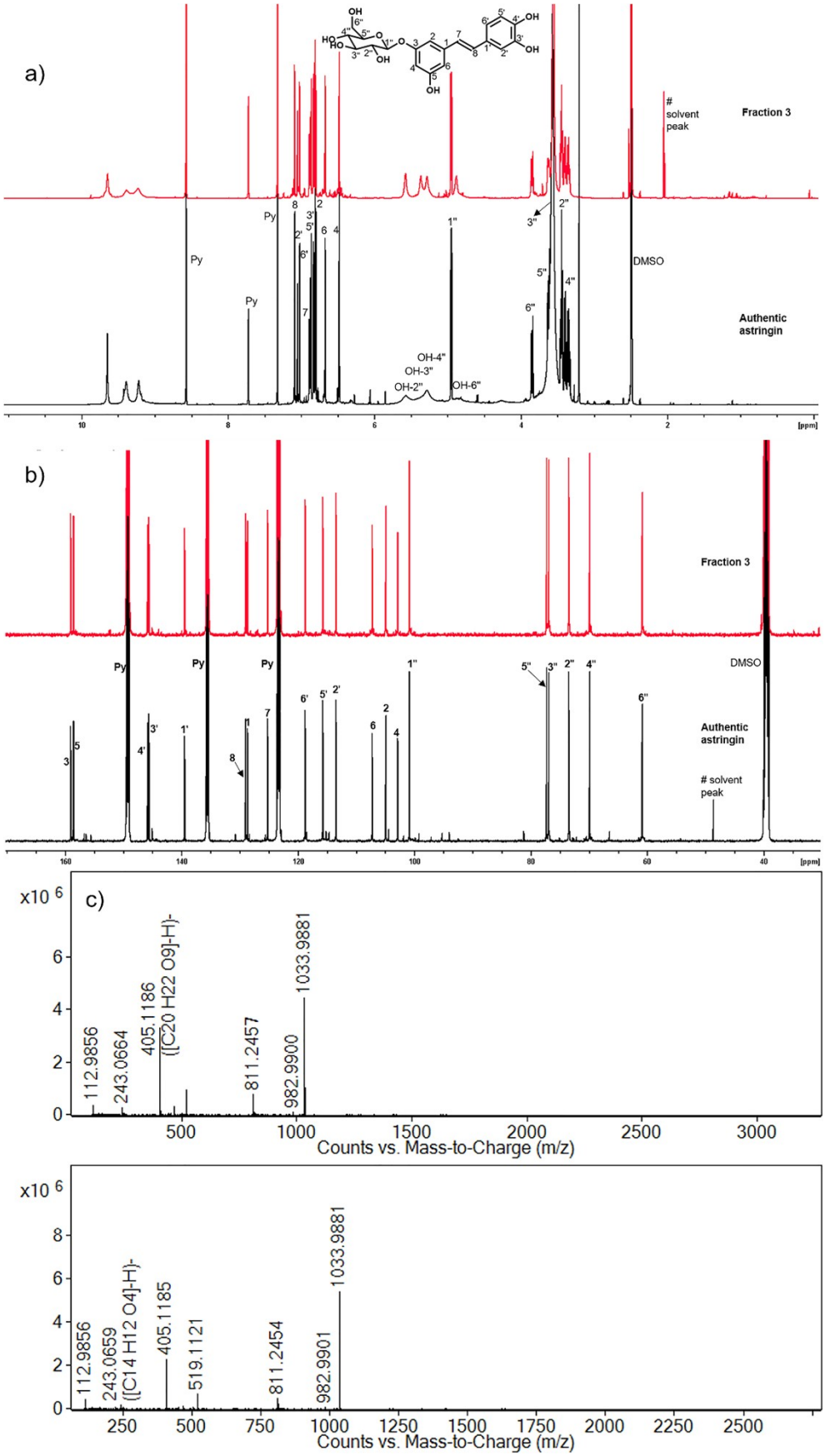

Fig. S8. a)^{1}H; b) ^{13}C NMR spectrum of **Fraction 3** (see **Fig. S2**) **and authentic astringin** in DMSO-*d*6/pyridine-*d*5; and c) HRMS spectrum (- ESI scan) of the **Fraction 3** (see **Fig. S2**) using the **column set I**.

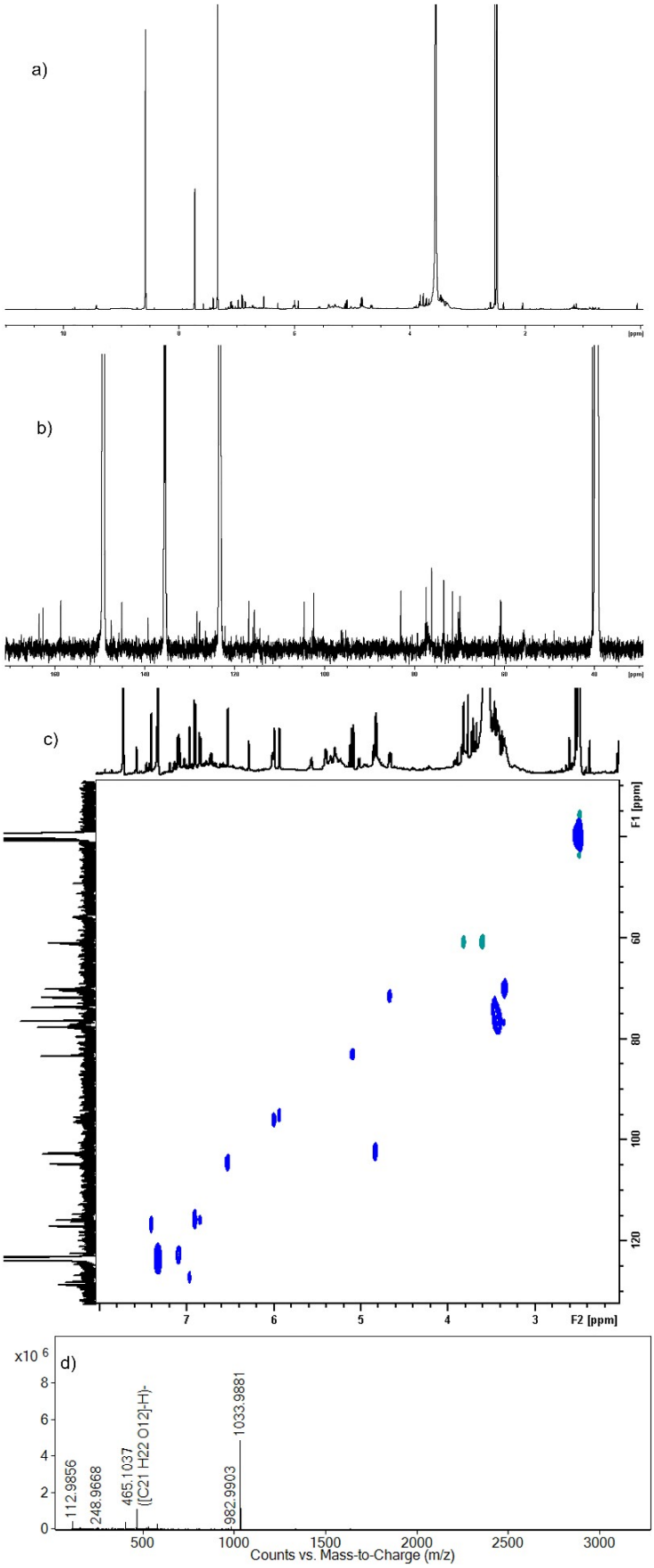

Fig. S9. a)^{1}H; b) ^{13}C; c) HSQC NMR spectrum of **Fraction 4** (see **Fig. S2**) in DMSO-*d*6/pyridine-*d*5; and d) HRMS spectrum (- ESI scan) of the **Fraction 4** (see **Fig. S2**) using the **column set I**.

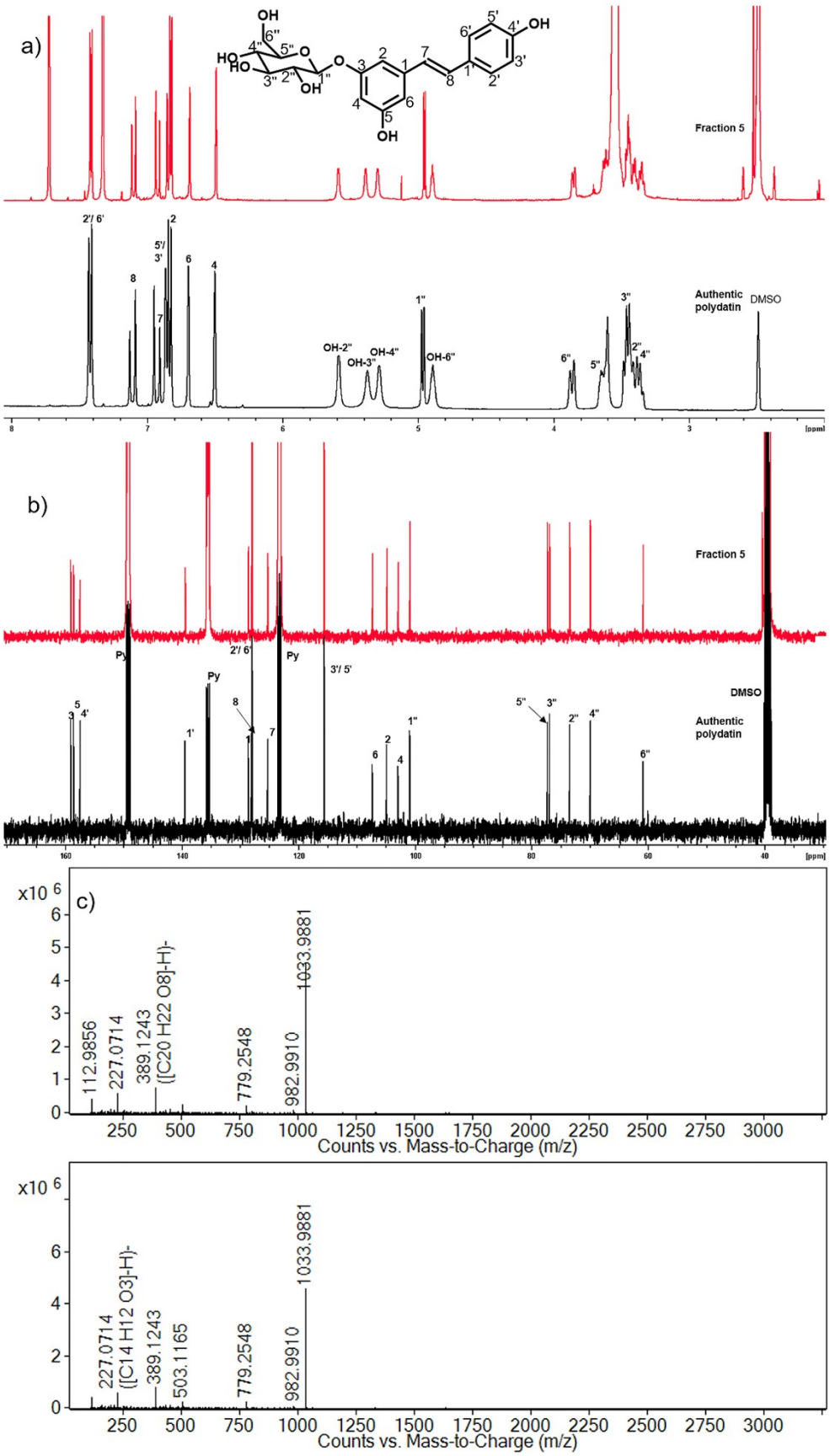

Fig. S10. a)[1]H; b) [13]C NMR spectrum of **Fraction 5** (see **Fig. S2**) **and authentic polydatin** in DMSO-*d*6/pyridine-*d*5; and c) HRMS spectrum (- ESI scan) of the **Fraction 5** (see **Fig. S2**) using the **column set I**.

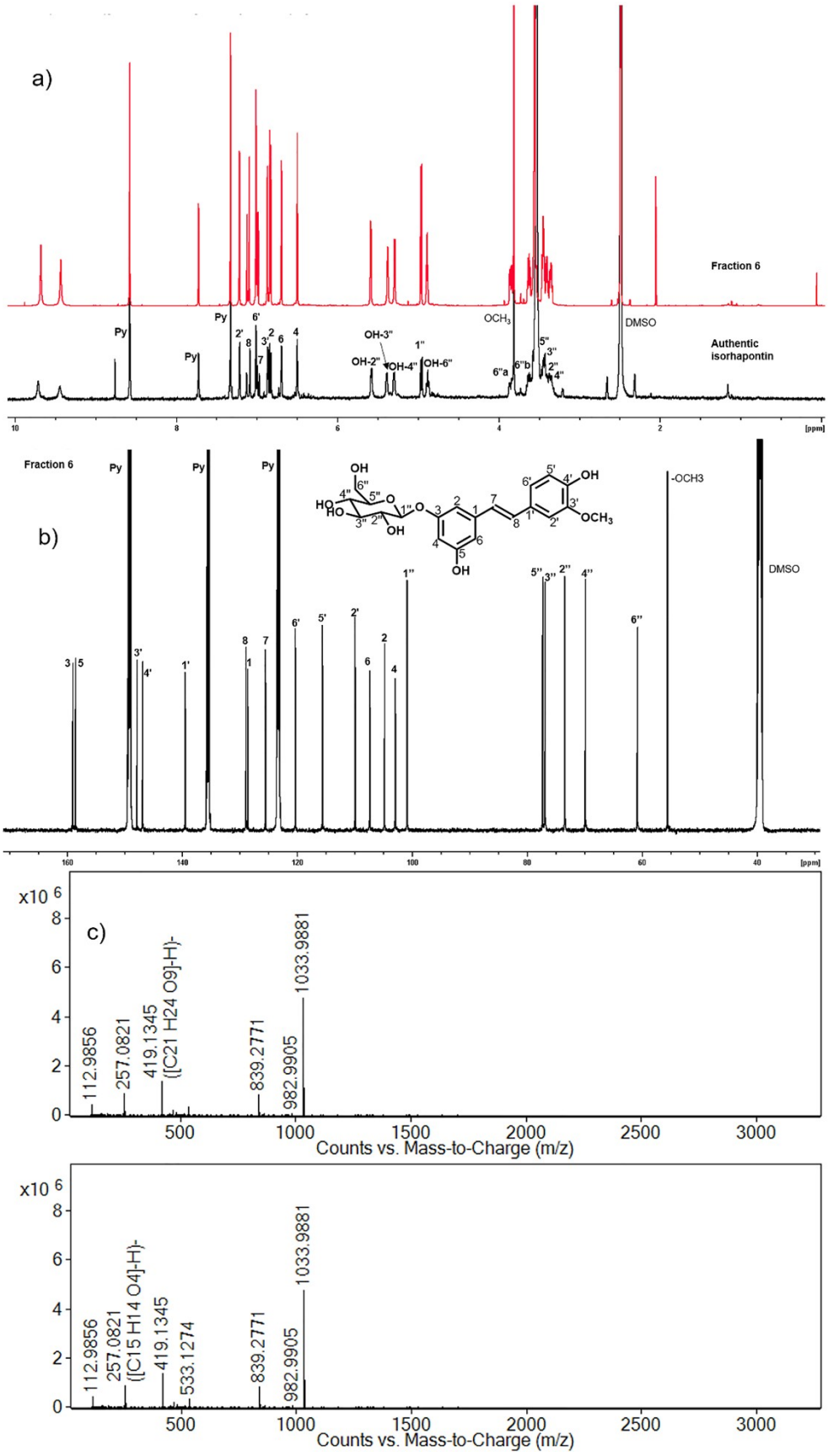

Fig. S11. a)[1]H NMR spectrum of **Fraction 6** (see **Fig. S2**) and authentic **Isorhapontin**; b) [13]C NMR spectrum of **Fraction 6** (see **Fig. S2**) in DMSO-*d*6/pyridine-*d*5; and c) HRMS spectrum (- ESI scan) of the **Fraction 6** (see **Fig. S2**) using the **column set I**.

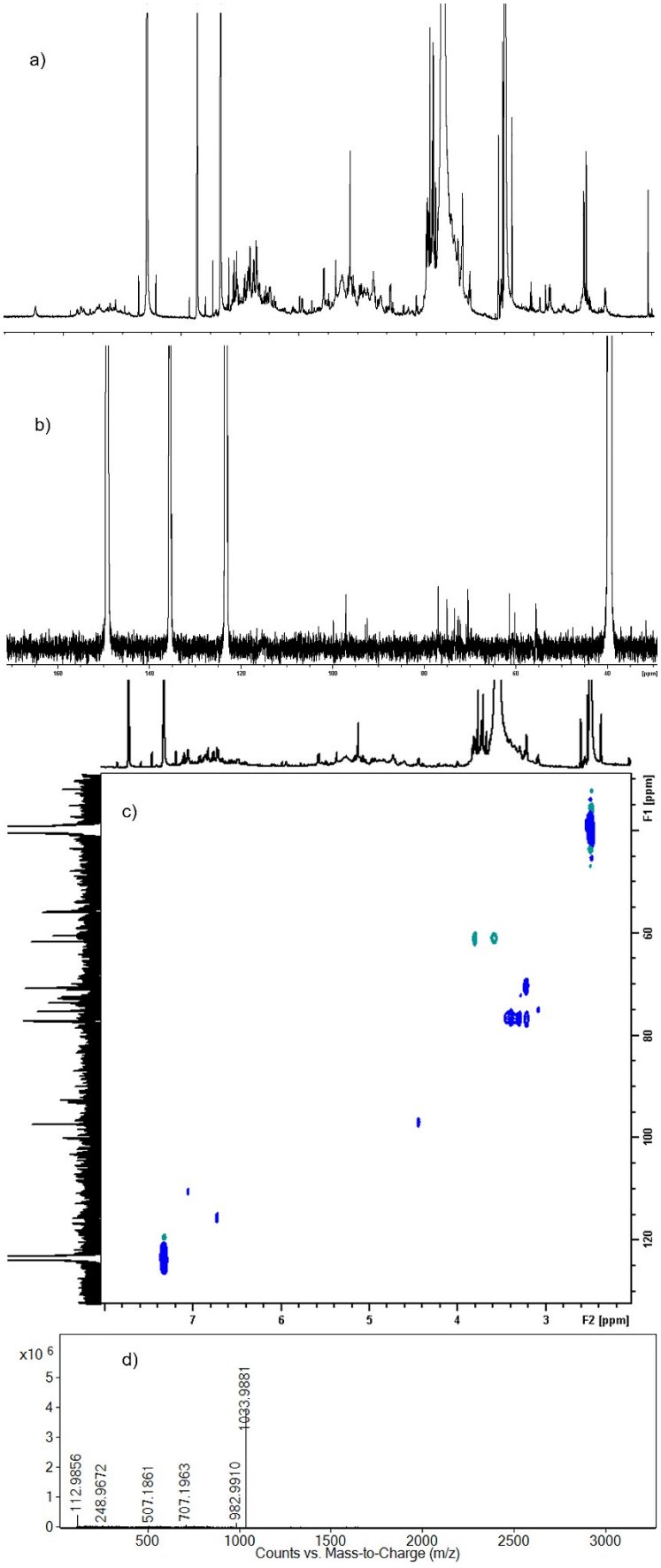

Fig. S12. a)^{1}H; b) ^{13}C; c) HSQC NMR spectrum of **Fraction 7** (see **Fig. S2**) in DMSO-*d*6/pyridine-*d*5; and d) HRMS spectrum (- ESI scan) of the **Fraction 7** (see **Fig. S2**) using the **column set I**.

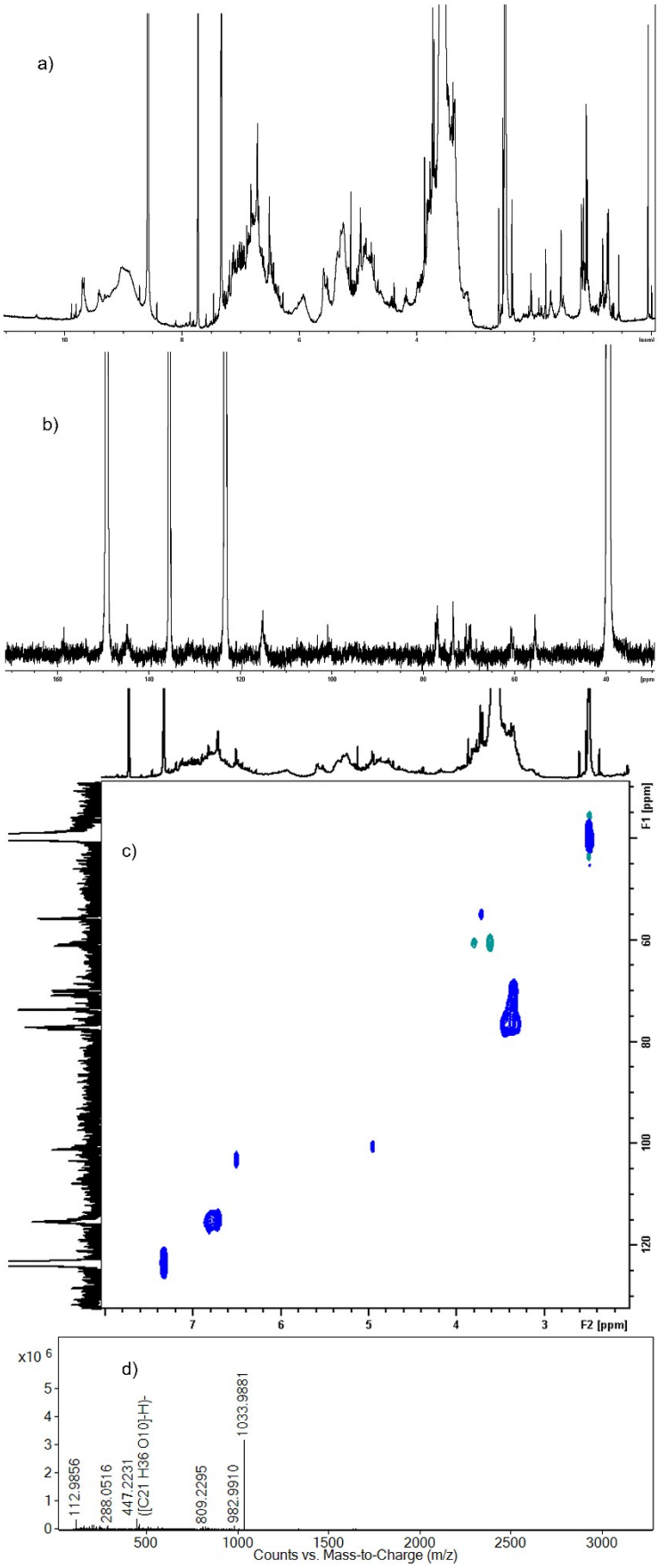

Fig. S13. a)[1]H; b) [13]C; c) HSQC NMR spectrum of **Fraction 8** (see **Fig. S2**) in DMSO-*d*6/pyridine-*d*5; and d) HRMS spectrum (- ESI scan) of the **Fraction 8** (see **Fig. S2**) using the **column set I**.

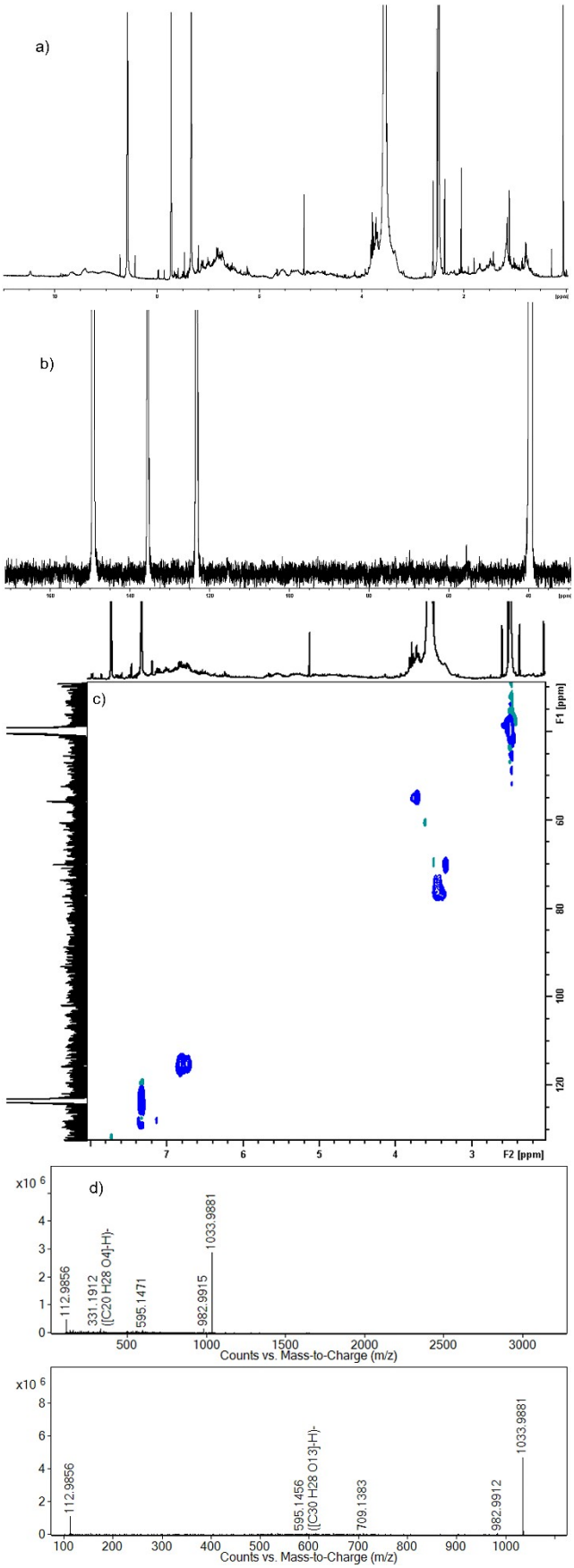

Fig. S14. a)^{1}H; b) ^{13}C; c) HSQC NMR spectrum of the **Fraction 9** (see **Fig. S2**) in DMSO-*d*6/pyridine-*d*5; and d) HRMS spectrum (- ESI scan) of the **Fraction 9** (see **Fig. S2**) using the **column set I**.

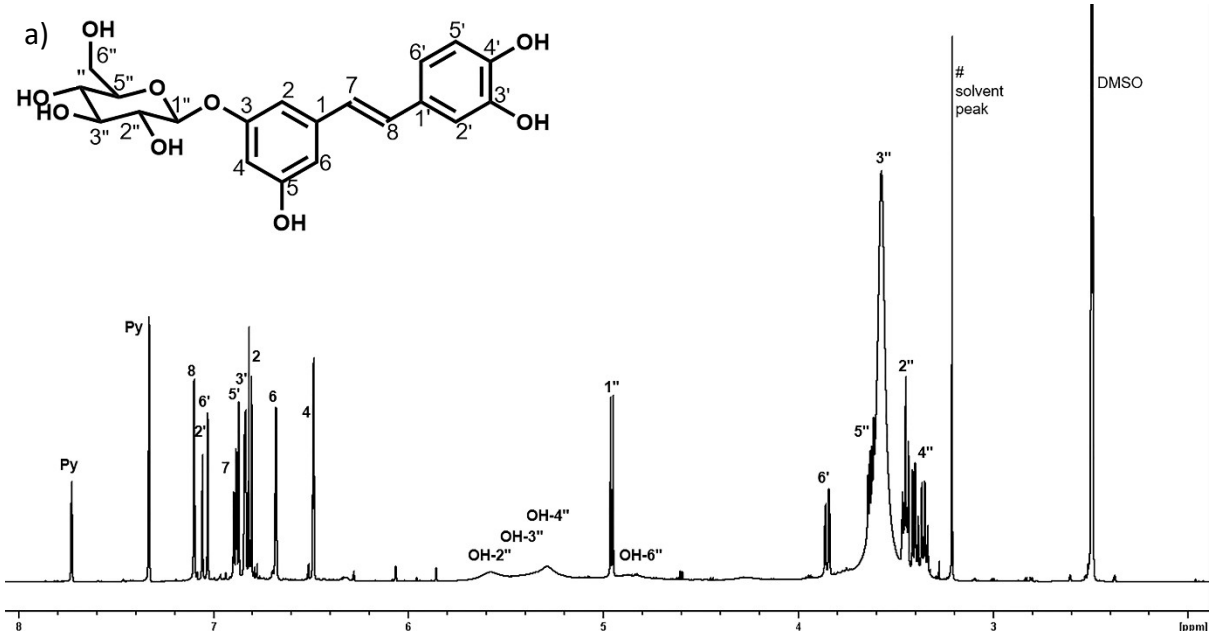
a)
OH
6"
5"
O
1"
O
HO
HO
3"
2"
OH
3
2
1
7
8
1'
2'
3'
4'
5'
6'
4
5
6
OH
OH
OH
Py
Py
8
6'
2'
7
5'
3'
2
6
4
OH-2"
OH-3"
OH-4"
1"
OH-6"
6'
5"
3"
2"
4"
solvent peak
DMSO
8
7
6
5
4
3
[ppm]

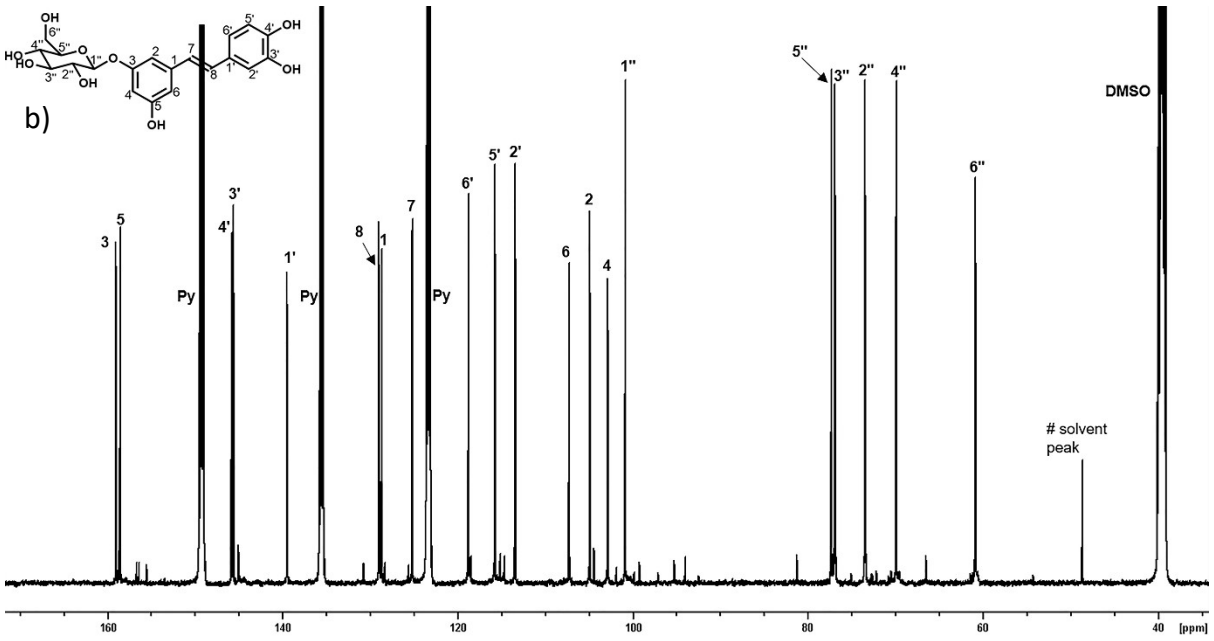
b)
OH
6"
4"
5"
O
1"
O
HO
HO
3"
2"
OH
3
2
1
7
8
1'
2'
3'
4'
5'
6'
4
5
6
OH
OH
OH
3
5
4'
3'
Py
1'
Py
8
1
7
Py
6'
5'
2'
6
2
4
1"
5"
3"
2"
4"
6"
DMSO
solvent peak
160
140
120
100
80
60
40
[ppm]

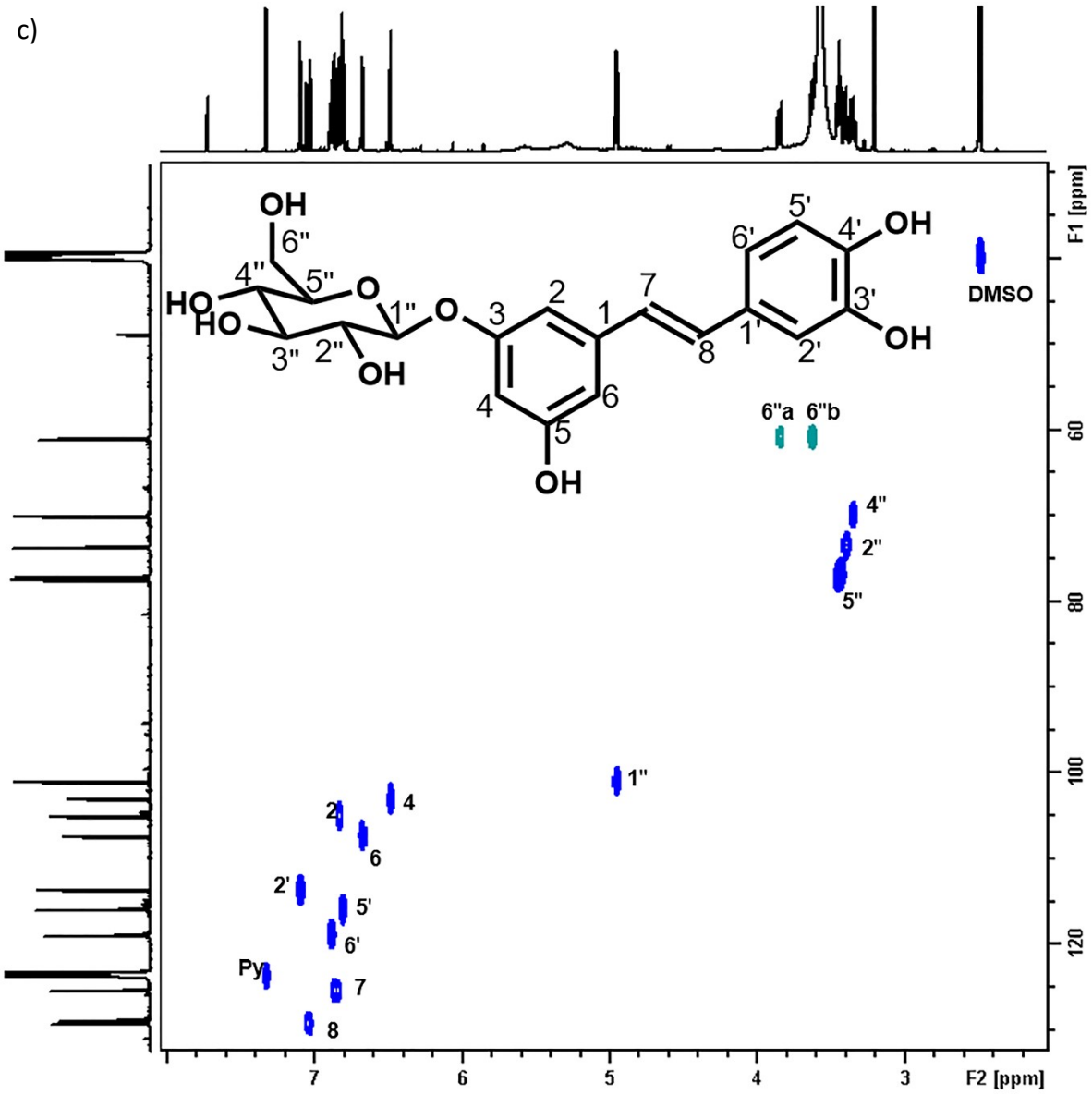

Fig. S15. a)^{1}H; b) ^{13}C; and c) 2D ^{1}H–^{13}C HSQC NMR spectrum of authentic Astringin 1 (see **Fig. 1)** in DMSO-*d*6/pyridine-*d*5.

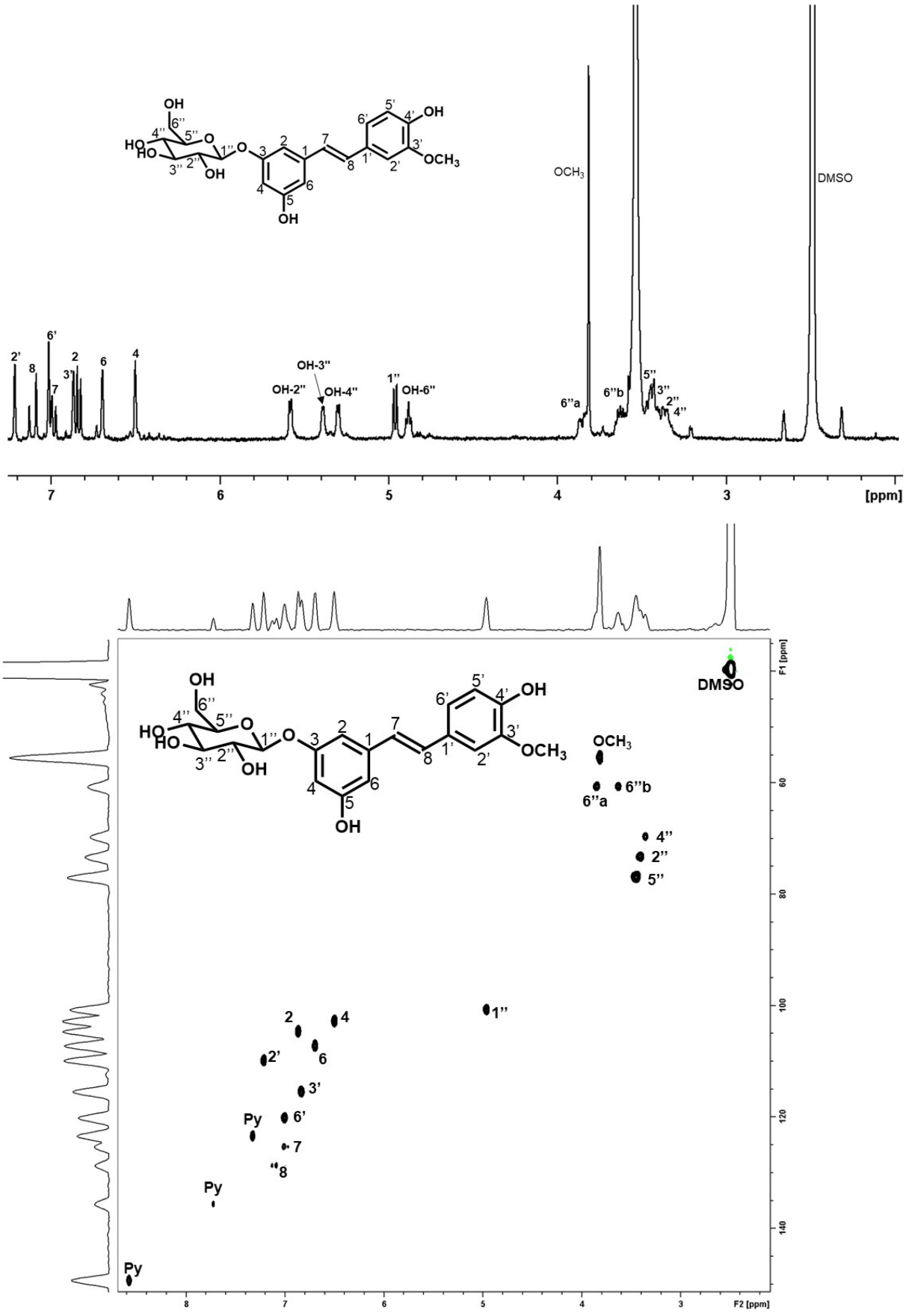

Fig. S16. ^{1}H (top) and 2D ^{1}H–^{13}C HSQC (bottom) NMR spectrum of authentic Isorhapontin 2 (see **Fig. 1)** in DMSO-*d*6/pyridine-*d*5.

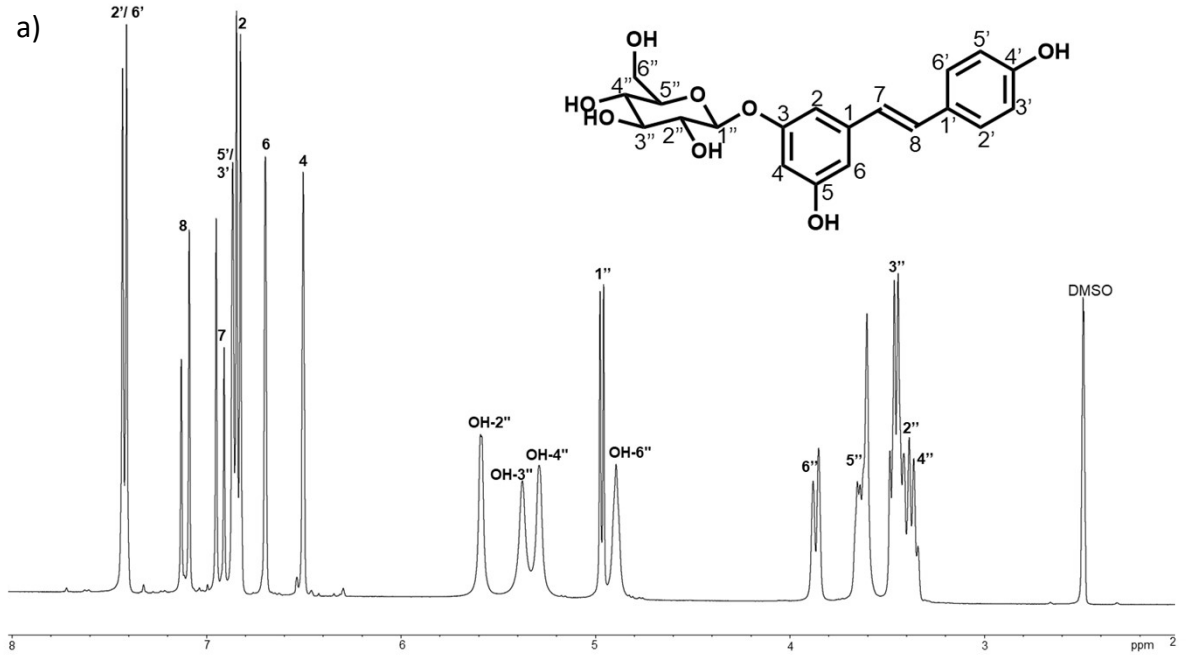
a)
2'/ 6'
2
5'/
3'
6
4
8
7
OH-2"
OH-3"
OH-4"
OH-6"
1"
6"
5"
2"
4"
3"
DMSO
OH
HO
HO
O
1
2
3
4
5
6
7
8
1'
2'
3'
4'
5'
6'
ppm

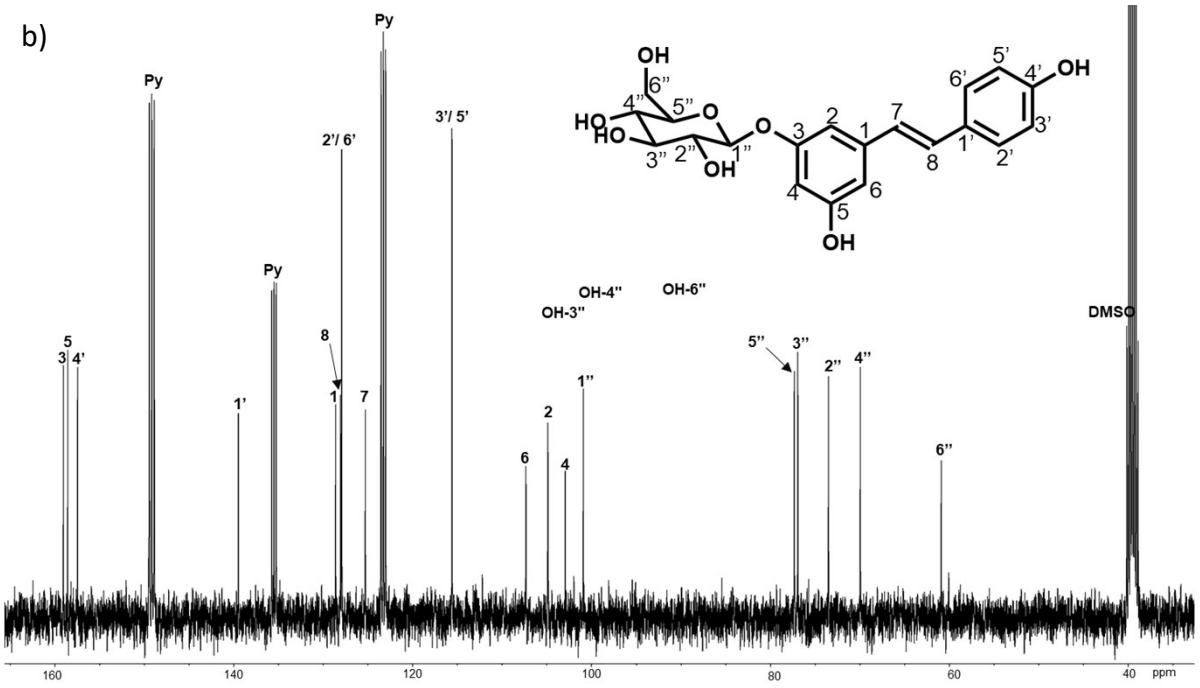
b)
Py
Py
Py
2'/ 6'
3'/ 5'
OH-3"
OH-4"
OH-6"
DMSO
5
3
4'
1'
8
1
7
6
2
4
1"
5"
3"
2"
4"
6"
OH
HO
HO
O
ppm

c)

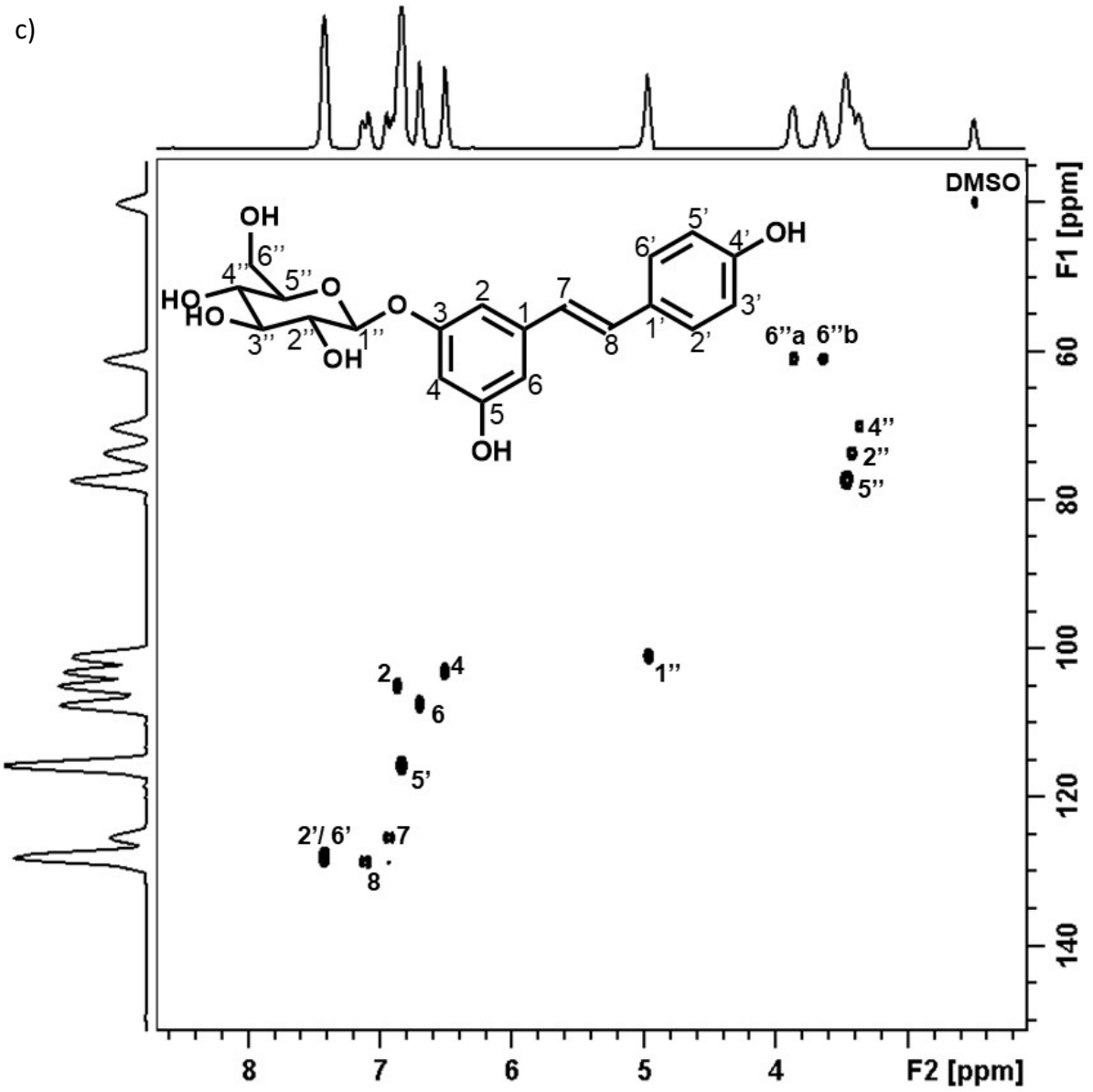

Fig. S17. a)^{1}H; b) ^{13}C; c) 2D ^{1}H–^{13}C HSQC NMR spectrum of authentic polydatin 3 (see **Fig. 1**) in DMSO-*d*6/pyridine-*d*5.

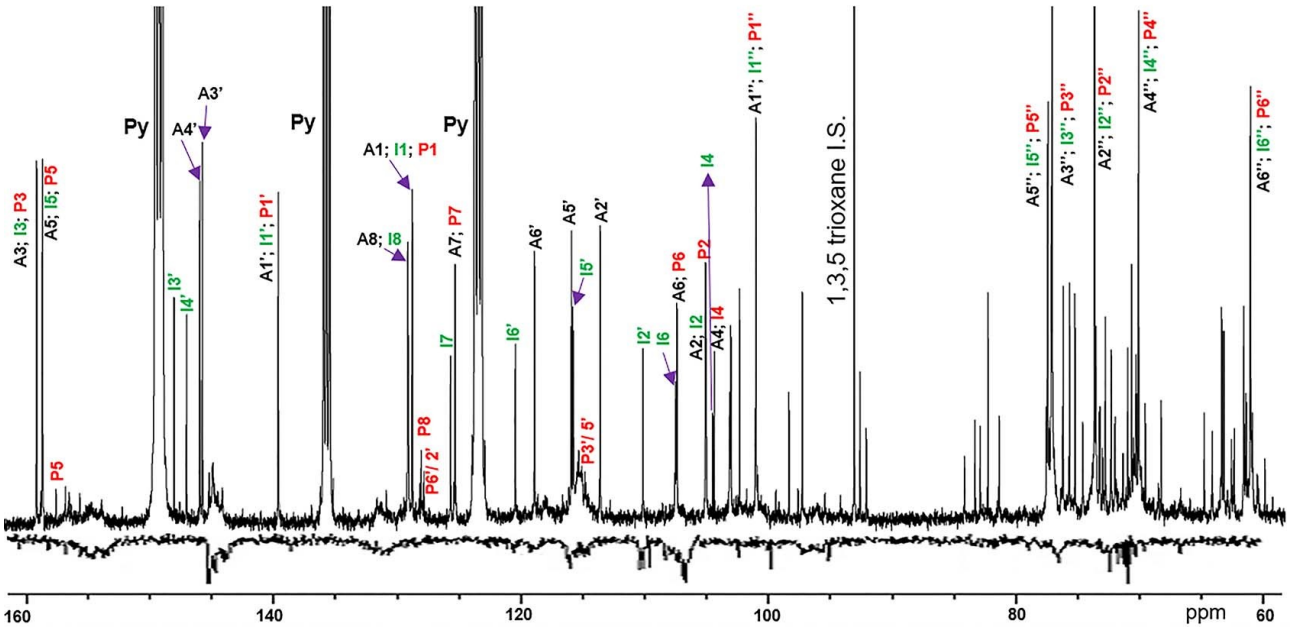

Fig. S18. Comparison between ^{13}C NMR spectra of spruce inner bark extract (**Fig. 1**) in DMSO-*d*6/pyridine-*d*5 and condensed tannin from leaves of *Leucaena leucocephala* hybrid Rendang in D_2O/acetone-*d*6 (1:1) (down, inverted).[1] The labels assign the signals from stilbene glucosides astringin (A, black), isorhapontin (I, green) and polydatin (P, red) (top).

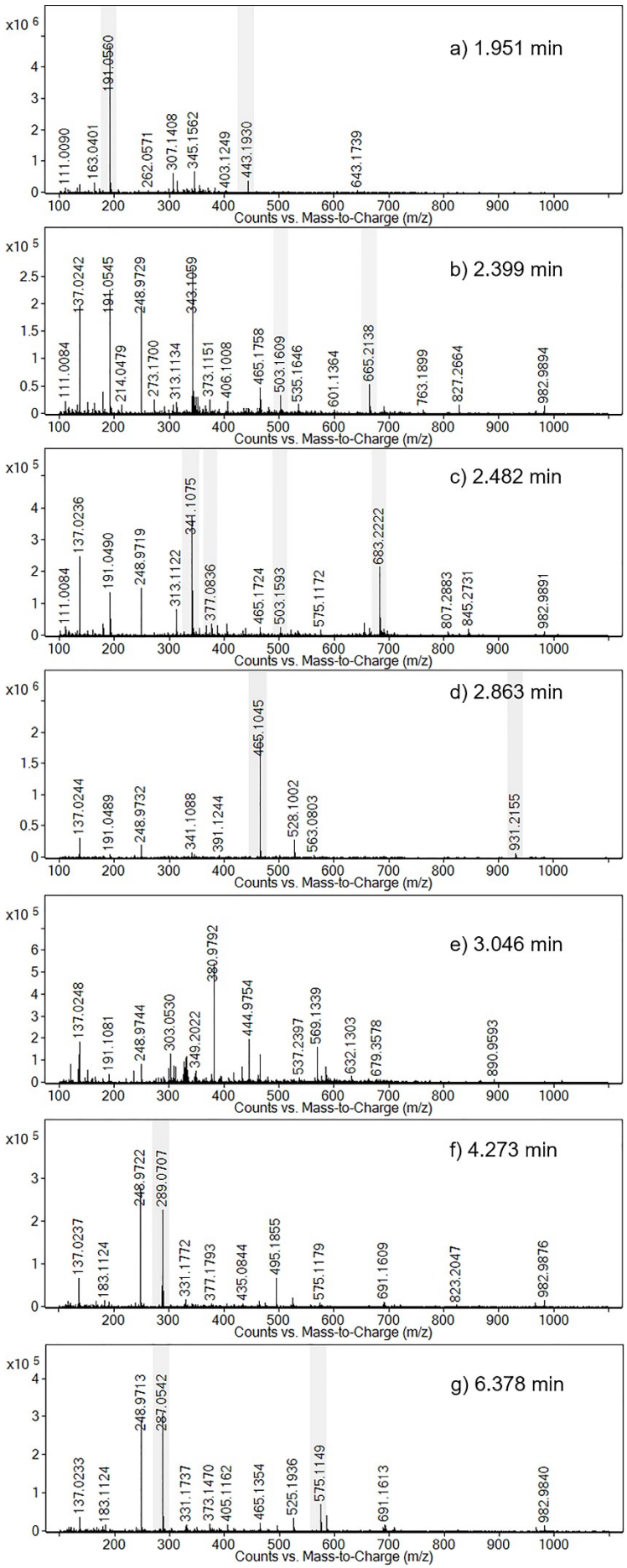
a) 1.951 min
x10 6
111.0090
163.0401
191.0560
262.0571
307.1408
345.1562
403.1249
443.1930
643.1739
b) 2.399 min
x10 5
111.0084
137.0242
191.0545
214.0479
248.9729
273.1700
313.1134
343.1059
373.1151
406.1008
465.1758
503.1609
535.1646
601.1364
665.2138
763.1899
827.2664
982.9894
c) 2.482 min
x10 5
111.0084
137.0236
191.0490
248.9719
313.1122
341.1075
377.0836
465.1724
503.1593
575.1172
683.2222
807.2883
845.2731
982.9891
d) 2.863 min
x10 6
137.0244
191.0489
248.9732
341.1088
391.1244
465.1045
528.1002
563.0803
931.2155
e) 3.046 min
x10 5
137.0248
191.1081
248.9744
303.0530
349.2022
380.9792
444.9754
537.2397
569.1339
632.1303
679.3578
890.9593
f) 4.273 min
x10 5
137.0237
183.1124
248.9722
289.0707
331.1772
377.1793
435.0844
495.1855
575.1179
691.1609
823.2047
982.9876
g) 6.378 min
x10 5
137.0233
183.1124
248.9713
287.0542
331.1737
373.1470
405.1162
465.1354
525.1936
575.1149
691.1613
982.9840
100
200
300
400
500
600
700
800
900
1000
Counts vs. Mass-to-Charge (m/z)

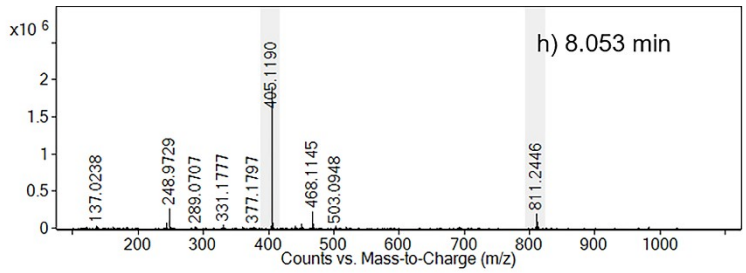
h) 8.053 min
x10 6
137.0238
248.9729
289.0707
331.1777
377.1797
405.1190
468.1145
503.0948
811.2446
Counts vs. Mass-to-Charge (m/z)

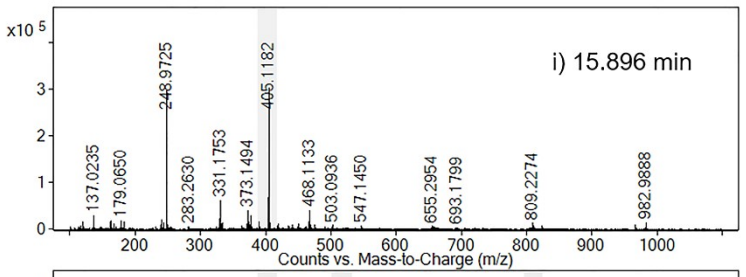
i) 15.896 min
x10 5
137.0235
179.0650
248.9725
283.2630
331.1753
373.1494
405.1182
468.1133
503.0936
547.1450
655.2954
693.1799
809.2274
982.9888
Counts vs. Mass-to-Charge (m/z)

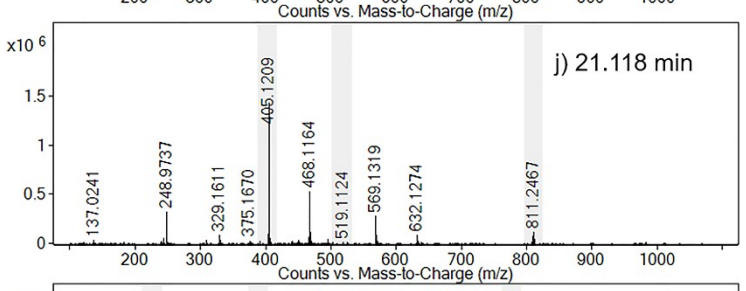
j) 21.118 min
x10 6
137.0241
248.9737
329.1611
375.1670
405.1209
468.1164
519.1124
569.1319
632.1274
811.2467
Counts vs. Mass-to-Charge (m/z)

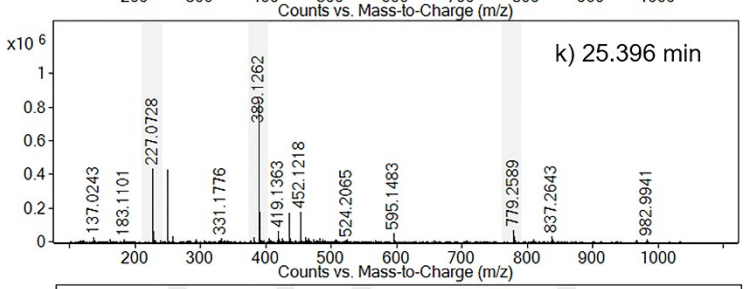
k) 25.396 min
x10 6
137.0243
183.1101
227.0728
331.1776
389.1262
419.1363
452.1218
524.2065
595.1483
779.2589
837.2643
982.9941
Counts vs. Mass-to-Charge (m/z)

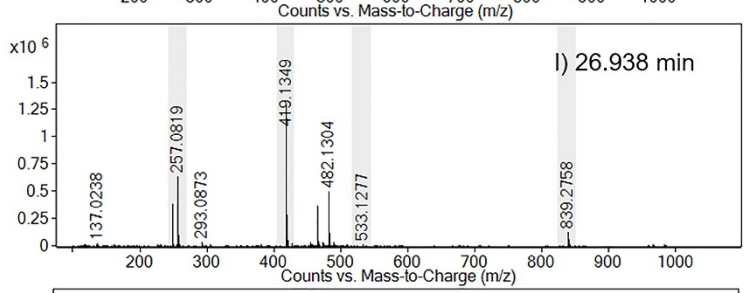
l) 26.938 min
x10 6
137.0238
257.0819
293.0873
419.1349
482.1304
533.1277
839.2758
Counts vs. Mass-to-Charge (m/z)

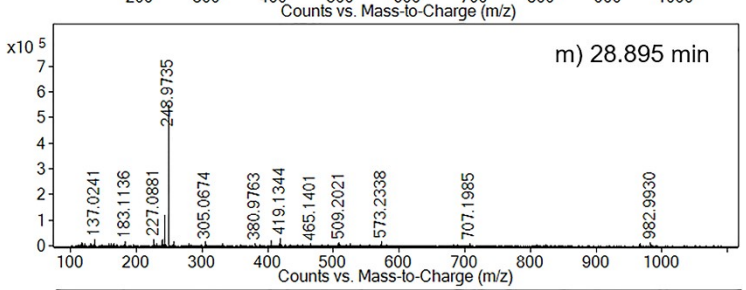
m) 28.895 min
x10 5
137.0241
183.1136
227.0881
248.9735
305.0674
380.9763
419.1344
465.1401
509.2021
573.2338
707.1985
982.9930
Counts vs. Mass-to-Charge (m/z)

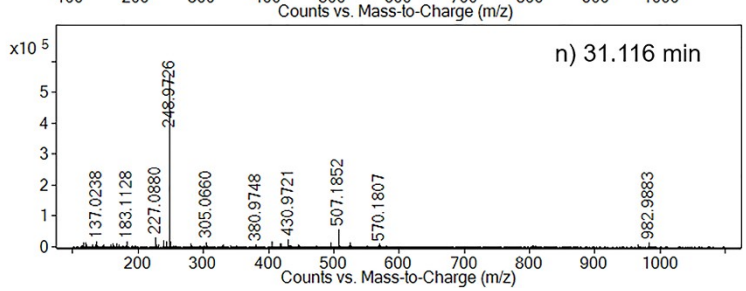
n) 31.116 min
x10 5
137.0238
183.1128
227.0880
248.9726
305.0660
380.9748
430.9721
507.1852
570.1807
982.9883
Counts vs. Mass-to-Charge (m/z)

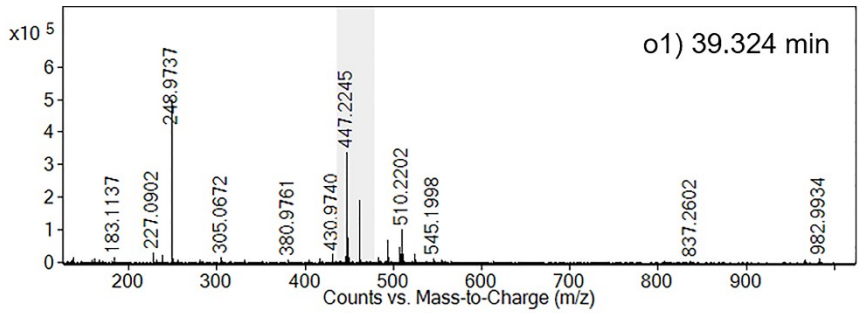
o1) 39.324 min
x10 5
248.9737
447.2245
183.1137
227.0902
305.0672
380.9761
430.9740
510.2202
545.1998
837.2602
982.9934
Counts vs. Mass-to-Charge (m/z)

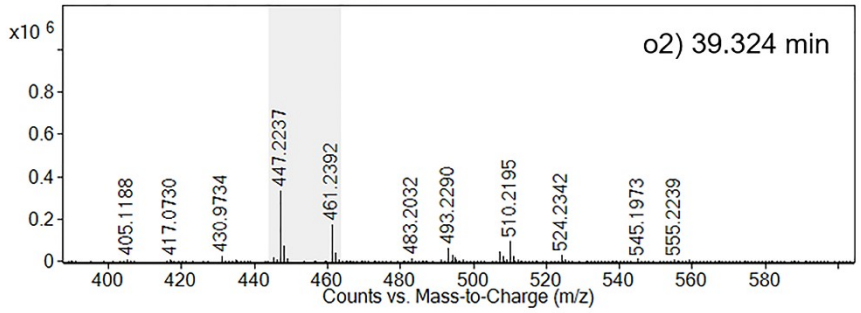
o2) 39.324 min
x10 6
447.2237
461.2392
405.1188
417.0730
430.9734
483.2032
493.2290
510.2195
524.2342
545.1973
555.2239
Counts vs. Mass-to-Charge (m/z)

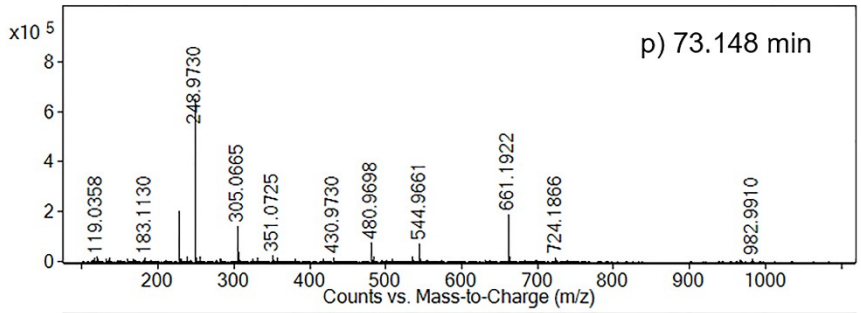
p) 73.148 min
x10 5
248.9730
119.0358
183.1130
305.0665
351.0725
430.9730
480.9698
544.9661
661.1922
724.1866
982.9910
Counts vs. Mass-to-Charge (m/z)

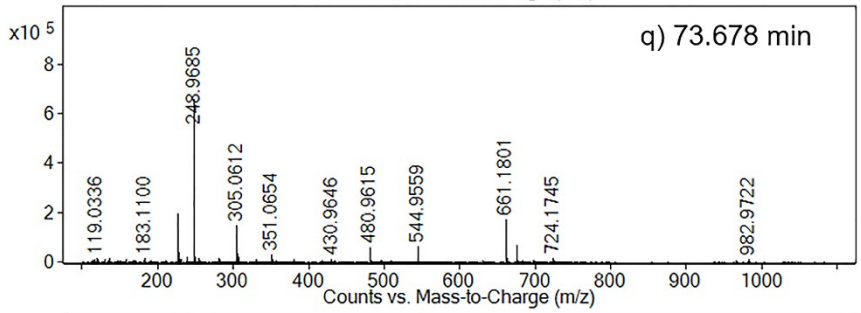
q) 73.678 min
x10 5
248.9685
119.0336
183.1100
305.0612
351.0654
430.9646
480.9615
544.9559
661.1801
724.1745
982.9722
Counts vs. Mass-to-Charge (m/z)

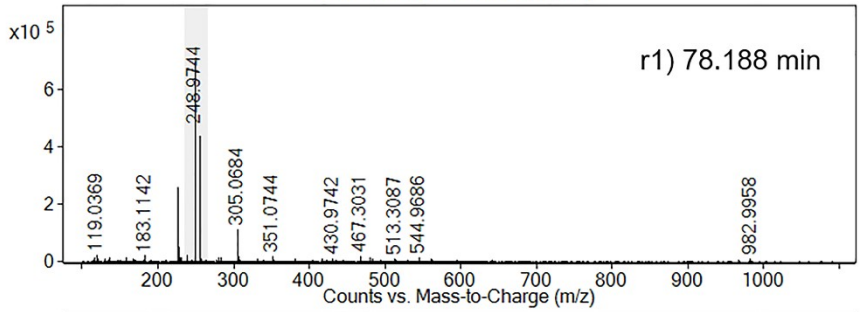
r1) 78.188 min
x10 5
248.9744
119.0369
183.1142
305.0684
351.0744
430.9742
467.3031
513.3087
544.9686
982.9958
Counts vs. Mass-to-Charge (m/z)

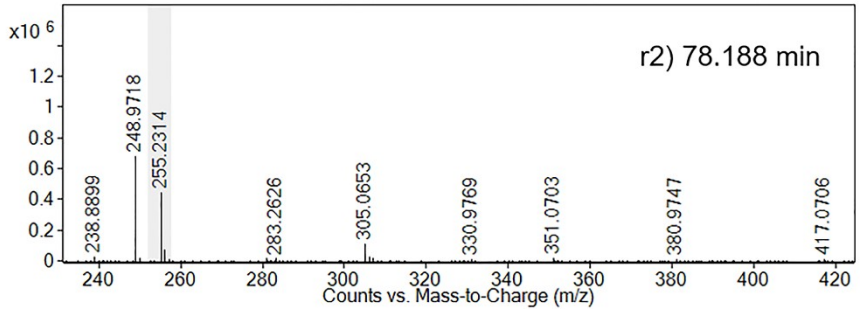
r2) 78.188 min
x10 6
248.9718
255.2314
238.8899
283.2626
305.0653
330.9769
351.0703
380.9747
417.0706
Counts vs. Mass-to-Charge (m/z)

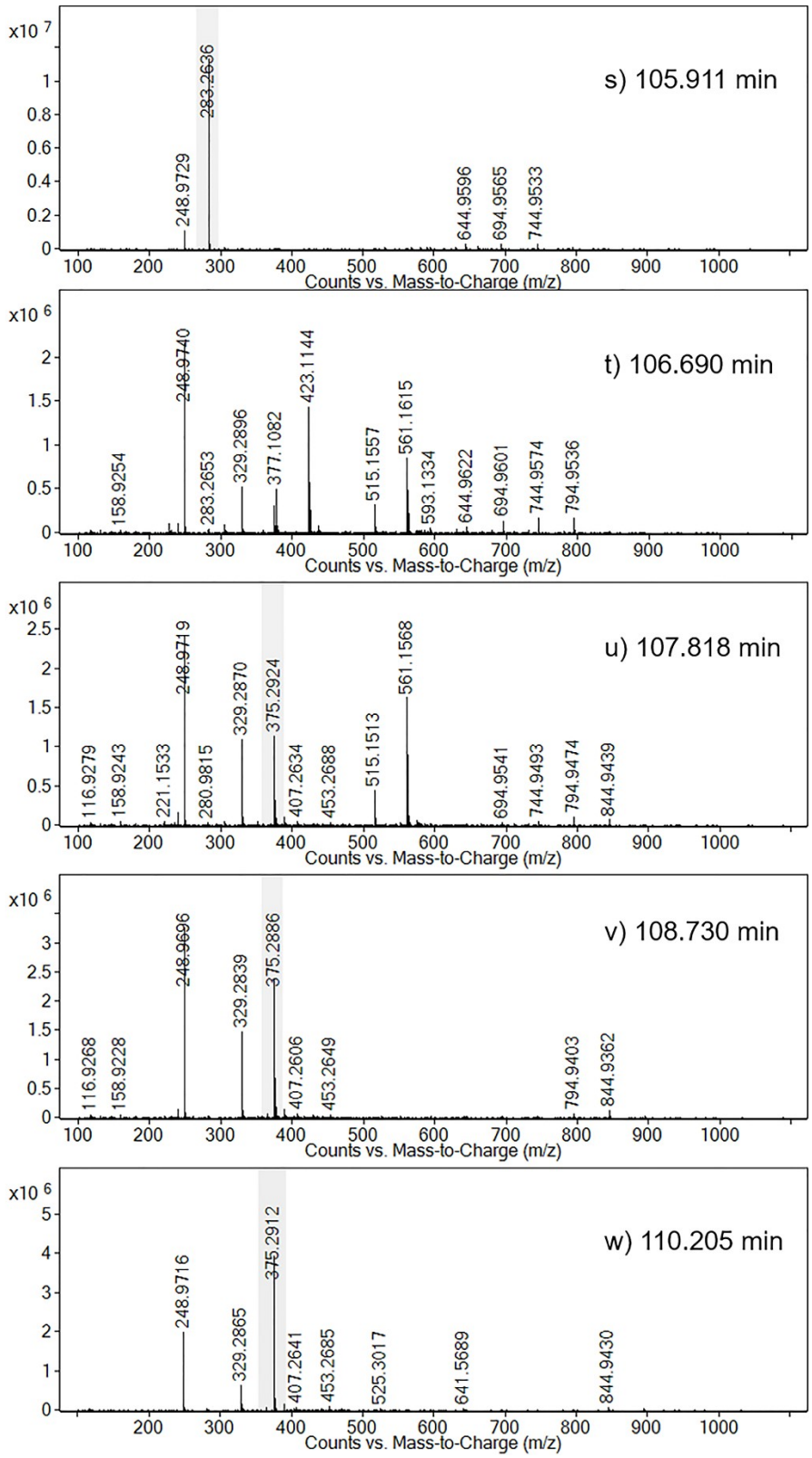

Fig. S19. The HRMS spectrum of spruce bark extract using the **column set II (**see **Table S2)** at the retention time of 1.951->3.046min (a->e, fraction 1); 4.273->6.378 min (f->g, fraction 2); 8.053 min (h, fraction 3); 15.896->21.118 min (i->j, fraction 4); 25.396 min (k, fraction 5); 26.938 min (l, fraction 6); 28.895-> 31.116 min (m->n, fraction 7); 39.324 min (o1-> o2, fraction 8); 106.690-> 110.205 min (t->w, fraction 9) and others (p->s, 73.148-> 105.911 min, refers to some uncollected fractions or baseline or impurities from the system).

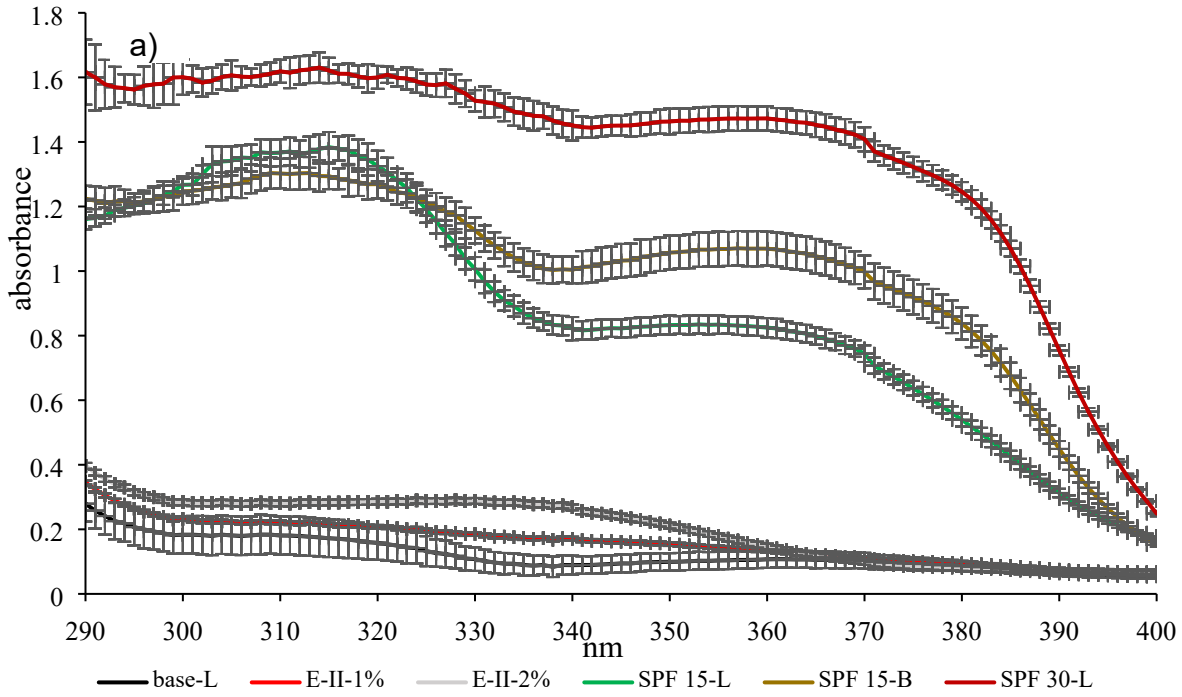
a)
absorbance
1.8
1.6
1.4
1.2
1
0.8
0.6
0.4
0.2
0
290
300
310
320
330
340
350
360
370
380
390
400
nm
base-L
E-II-1%
E-II-2%
SPF 15-L
SPF 15-B
SPF 30-L

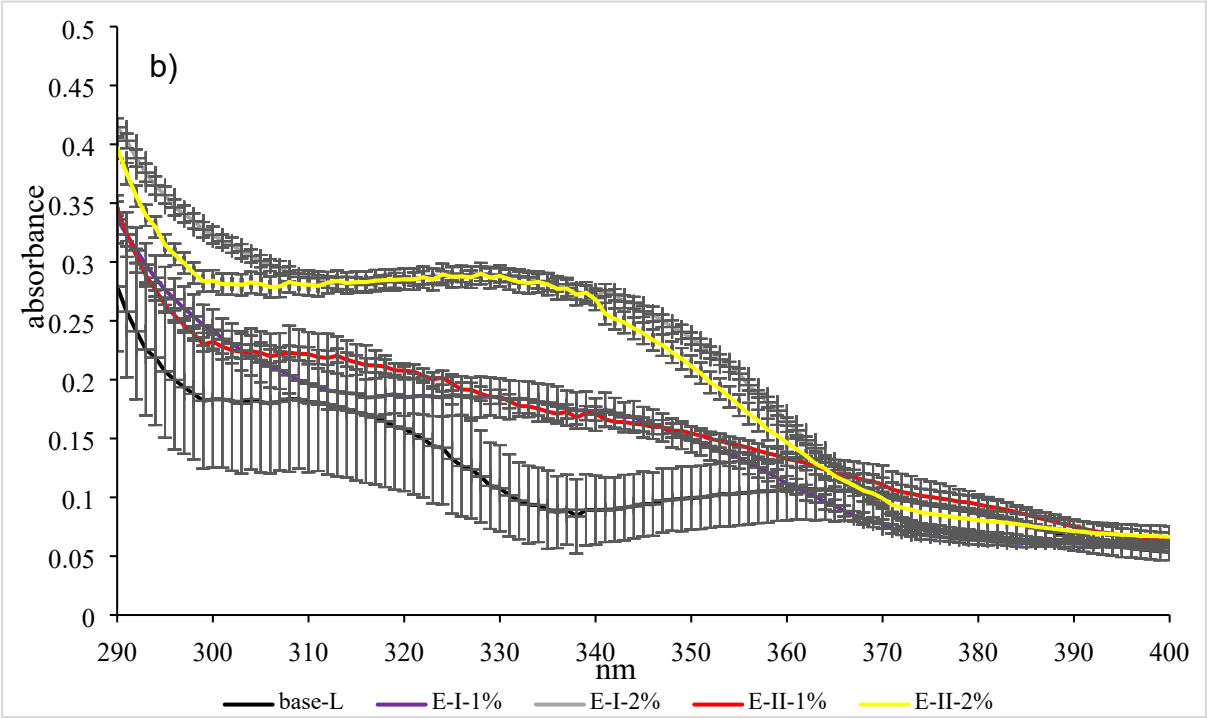
b)
absorbance
0.5
0.45
0.4
0.35
0.3
0.25
0.2
0.15
0.1
0.05
0
290
300
310
320
330
340
350
360
370
380
390
400
nm
base-L
E-I-1%
E-I-2%
E-II-1%
E-II-2%

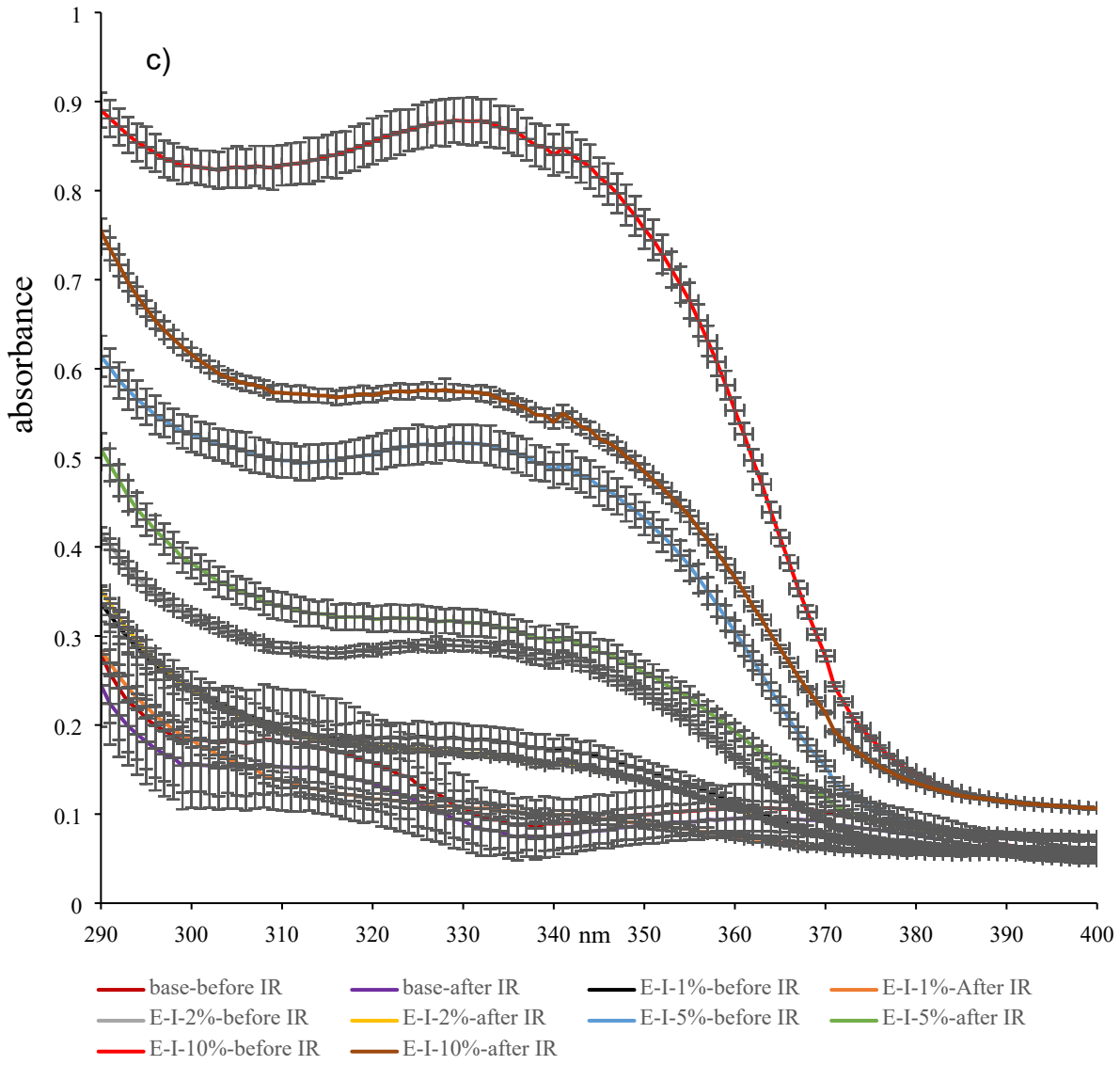

Fig. S20. UVA–UVB absorbance (290–400 nm) of sunscreens from a) emulsification II (E-II-1% and E-II-2%, respectively) in comparison to the commercial creams (15-L; SPF 15-B; and SPF 30-L); b) emulsification II (E-II-1% and E-II-2%, respectively) in comparison to emulsification I (E-I-1% and E-I-2%, respectively); and c) emulsification I (E-I-1%, E-I-2%, E-I-5%, E-I-10%, and base cream, respectively) before the solar irradiation in comparison to their emulsions after the solar irradiation. Their standard deviations are included. base-L is applied here as the reference.

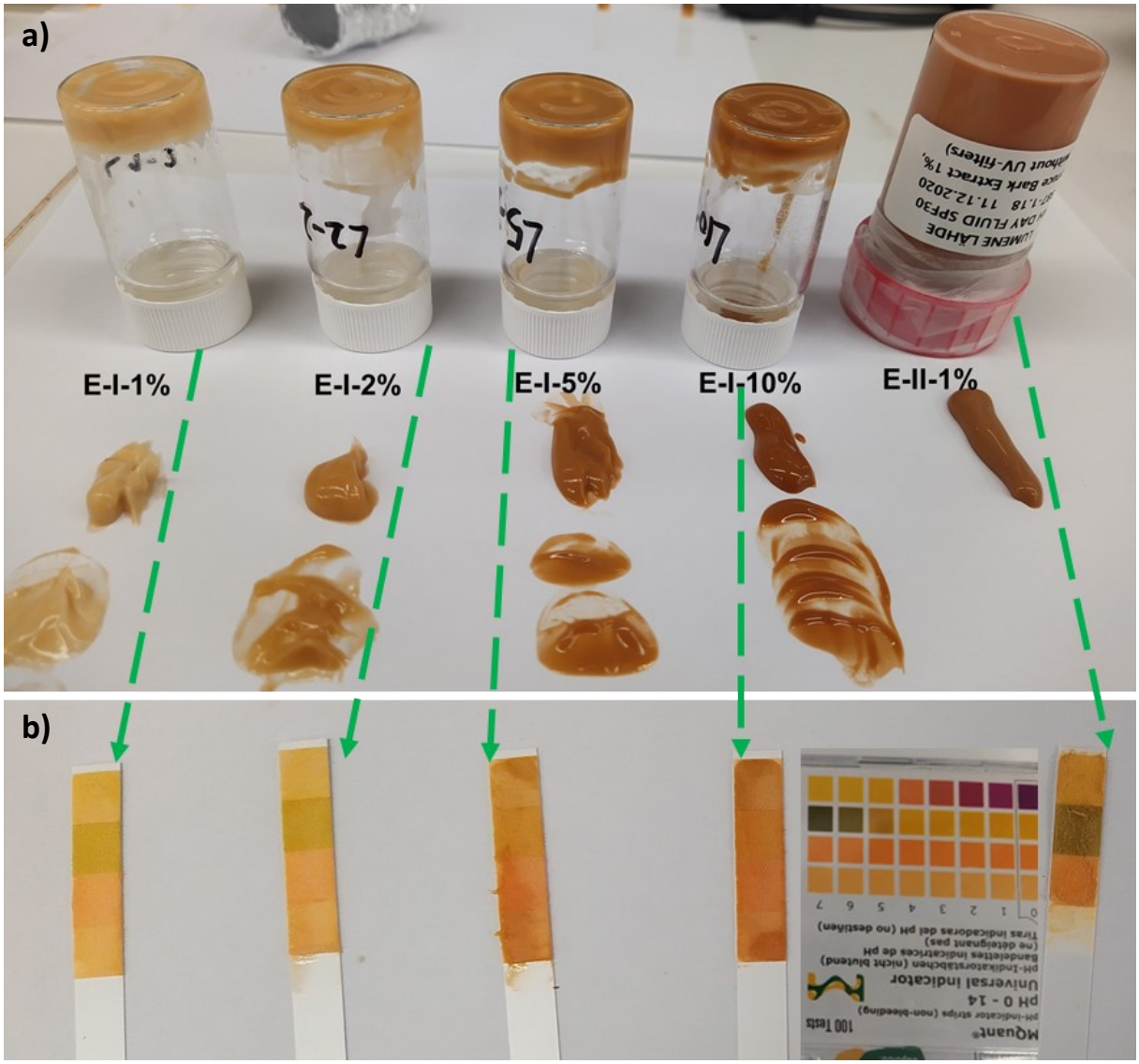

Fig. S21. Photographs of sunscreens from emulsification I (E-I-1%, E-I-2%, E-I-5%, and E-I-10%, respectively) in comparison to the emulsification II (i.e.E-II-1%): a) visual differences; b) pH differences as indicated by the pH meter indicator.

References

1 M. A. Zarin, H. Y. Wan, A. Isha and N. Armania, *Food Sci. Hum. Wellness*, 2016, **5**, 65–75. https://doi.org/10.1016/j.fshw.2016.02.001.